Nature Reviews Earth & Environment
January 2024, Volume 5 Pages 23-42
https://doi.org/10.1038/s43017-023-00502-0
https://archimer.ifremer.fr/doc/00871/98258/

Wind-wave climate changes and their impacts

Casas-Prat Mercè [1,*], Hemer Mark A. [2], Dodet Guillaume [3], Morim Joao [4], Wang Xiaolan L. [1], Mori Nobuhito [5], Young Ian [6], Erikson Li [7], Kamranzad Bahareh [8], Kumar Prashant [9], Menéndez Melisa [10], Feng Yang [1]

[1] Environment and Climate Change Canada, Climate Research Division, Science and Technology Branch, Toronto, Ontario, Canada
[2] CSIRO Environment, Hobart, Tasmania, Australia
[3] Univ. Brest, CNRS, IFREMER, IRD, Laboratoire d'Océanographie Physique et Spatiale, Brest, France
[4] Coastal Risks and Engineering Lab, University of Central Florida, Orlando, FL, USA
[5] Disaster Prevention Research Institute, Kyoto University, Kyoto, Japan
[6] Department of Infrastructure Engineering, University of Melbourne, Parkville, Victoria, Australia
[7] US Geological Survey, Pacific Coastal and Marine Science Center, Santa Cruz, CA, USA
[8] Department of Civil and Environmental Engineering, University of Strathclyde, Glasgow, UK
[9] Department of Applied Sciences, National Institute of Technology, Delhi, India
[10] Environmental Hydraulics Institute (IHCantabria), Universidad de Cantabria, Santander, Spain

* Corresponding author : Mercé Casas-Prat, email address : merce.casasprat@ec.gc.ca

Abstract :

Wind-waves have an important role in Earth system dynamics through air–sea interactions and are key drivers of coastal and offshore hydro-morphodynamics that affect communities, ecosystems, infrastructure and operations. In this Review, we outline historical and projected changes in the wind-wave climate over the world's oceans, and their impacts. Historical trend analysis is challenging owing to the presence of temporal inhomogeneities from increased numbers and types of assimilated data. Nevertheless, there is general agreement over a consistent historical increase in mean wave height of 1–3 cm yr−1 in the Southern and Arctic Oceans, with extremes increasing by >10 cm yr−1 for the latter. By 2100, mean wave height is projected to rise by 5–10% in the Southern Ocean and eastern tropical South Pacific, and by >100% in the Arctic Ocean. By contrast, reductions in mean wave height up to 10% are expected in the North Atlantic and North Pacific, with regional variability and uncertainty for changes in extremes. Differences between 1.5 °C and warmer worlds reveal the potential benefit of limiting anthropogenic warming. Resolving global-scale climate change impacts on coastal processes and atmospheric–ocean–wave interactions requires a step-up in observational and modeling capabilities, including enhanced spatiotemporal resolution and coverage of observations, more homogeneous data products, multidisciplinary model improvement, and better sampling of uncertainty with larger ensembles.

Keywords : Climate change, Physical oceanography, Projection and prediction

Introduction

Differential heating of the earth's surface drives winds across the ocean surface, that in-turn transfer some of their energy to the water in the form of surface ocean wind-waves[1], also called surface gravity waves[2]. At any point, the wind-wave field is a spectrum of superimposed waves generated by winds from several distributed weather systems that have met at that point in space and time, including the locally generated wind sea states and the long-travelled swells[2]. The combination of these wind-wave systems define altogether the sea state, which is considered an Essential Ocean Variable (EOV) and an Essential Climatic Variable (ECV) by the Global Ocean Observing System (GOOS) and the World Meteorological Organization (WMO), respectively. It is well established that wind-waves respond to changes in atmospheric circulation (wind speed, direction, and duration), and changes in fetch (for example, with changes in sea-ice distribution)[3]. Wind-waves can also be modulated by intense currents[4] and strong nearshore bathymetric gradients[5]. Wind-waves are dominant contributors to coastal hydro-morphodynamics[6,7] and have an important role in navigation and offshore industry[8]. Also, they are a potential source of renewable marine energy[9–11], which could contribute to the development of sustainable blue economy[12,13].

Natural and anthropogenically-forced climate variability drive changes in wind-waves, that can be experienced as changes in wave height, period (or wave-length), energy (or power), and/or the direction in which they travel[14]. The resultant changes in the wind-wave climatology have important consequences, with influence on marine and coastal engineering, industrial operations, and environmental management. For example, future changes in wind-waves might exacerbate coastal erosion[15–18], and flooding[15,19,20], affect the stability of (largerly expanding[21]) marine-built infrastructure[22], threaten the safety of offshore operations[23], and disrupt coastal ecosystems[24]. Furthermore, changes in wind-wave characteristics may drive potential feedback to the climate system through modulation of fluxes across the air-sea interface, wave-ice interactions, or other processes[25,26].

Following the fourth assessment report (AR4) of the United Nations (UN) Intergovernmental Panel for Climate Change (IPCC)[27], which highlighted low confidence in future ocean wave climate projections, interest in historical and projected changes in wind-wave climate has received much attention – at least in part driven by the interests of the WMO supported Coordinated Ocean Wave Climate Project (COWCLIP)[28]. Implications of historical and future wind-wave climate change extend from global down to local scales, and there is now a large body of literature that span this space and time-scales. Coordinated activities assessing historical change at the global scale (for example, through the European Space Agency Sea State Climate Change Initiative[29], the Copernicus Marine Service[30], global wave hindcasts/reanalysis[31], and other global data products[32]) and community ensembles of global wave climate projections[33–38] have improved the perspective of wave climate change at the global scale. Meanwhile, there have been many studies investigating wave climate change at local to regional scales with existing local and regional studies unevenly spanning the world oceans/seas[34]. This increase in the body of literature is reflected in the IPCC's AR6[39], which indicates medium confidence for the projections of changes in mean wave climate but confidence in extreme wave conditions remains low.

In this review, we build a global perspective of historical and future projected wind-wave climate change, piecing together evidence from local, regional, and global studies. We begin by presenting a general overview of the state-of-the-art methods and datasets, while identifying key challenges. Next, we synthesize the main features of the historical and future wind-waves by ocean basin, including their relations with atmospheric teleconnection patterns. We also provide illustrative examples of implications of wind-wave changes. We end with a summary and discussion of perspectives for future research.

Data, methods and key challenges

With existing research now expanding several decades, we possess a solid understanding of the main features of the historical wind-wave climate and potential future changes in a warmer world. However, there are still significant uncertainties related to our observational and modelling capabilities despite continuous improvements. In this section, we present an overview of the main available datasets and methods to study historical and future wave conditions, as well as the associated limitations and challenges.

Historical wave climate

The wind-wave climatology has received particular attention since the second half of the 20th century. The North Atlantic was a first focus for wind-wave climate research[40] as military operations, oil exploration, and shipping activities between Europe and the US required a detailed understanding of sea state variability. Increasingly, deployment of in-situ wave observations (wave buoys), coordination of voluntary observing ship (VOS) records of sea state[41], the availability of regional and global scale wind-wave hindcasts and reanalyses, and satellite observations (primarily altimeter, with increasing exploitation of other sensors such as Synthetic Aperture Radars, SAR, and wave spectrometer[42,43]), have provided longer and more suitable datasets for deriving wind-wave climatology and its variability over the global oceans over at least a few decades[29,32,44], and are critical supplements to study the regional wave climate.

Despite the substantial increase in wave observations over the last years, their temporal and spatial coverage remains heterogeneous, and long wave records are scarce. For instance, moored buoys are mostly located in the North Hemisphere and just a small fraction of them exceeds 40 years of data (Fig. 1(a)). Additionally, observations are affected by temporal inhomogeneities[45] due to changes in network characteristics over time (for example, device modernization, relocation, increase in sampling frequency) and quality control and postprocessing procedures. In general, temporal inhomogeneities can be defined as temporal variations or discontinuities in observed records (or climate products that assimilate observations) that result from non-climatic factors such as changes in the way the measurements were performed. With now more than 30 years of data (Fig. 1(b)), satellite remote sensing offers valuable information. However, differences in multi-mission calibration procedures can lead to differences in resulting climatological values, and, particularly, trends[44,46] (Figs. 2(a) and S1). Moreover, its sparse sampling pattern leads to undersampling errors that particularly affect the extremes of earlier periods with a lower amount of in-orbit altimeters[47]. For example, only one altimeter mission (GEOSTAT) was in orbit over 1985-1990[32] (with the next mission starting late 1991), whereas 8 altimeter missions were in orbit in 2020[48]. One promising way to supplement altimetry undersampling could stem from the combined use of SAR missions. Despite a lower SAR wave mode acquisition rate (∼100km) compared to the 1Hz altimeter data (∼7km), the wave spectral information derived from SAR images can be used to propagate swell properties along great circles from their source regions to the coastline[49], and therefore increase the wave population density.

To overcome the limitations associated with observations, wave hindcasts and reanalyses[30,31] are often used as observation *proxies* (wave hindcasts do not assimilate wave observations but both wave reanalysis and hindcast products indirectly account for assimilated atmospheric observations). They are invaluable tools that have helped advance understanding of the historical wave climate at global and regional scales. Wave hindcasts/reanalysis and satellite data have also been used to demonstrate the relation between global wave characteristics and leading teleconnection patterns that are known to be closely associated with general climate variability over multiple time-scales[50–52]. Existing literature has largely focused on integrated wave parameters such as the significant wave height (H_s), the mean wave period (T_m) and the mean wave direction (θ_m) (see Box 1), with a limited amount of wave products developed for the full wave spectrum[53].

Existing research provides no clear evidence about what wave product can be used as a gold standard, and performance often varies depending on the region of interest[54]. Multi-product ensembles can be used to identify common features and assess uncertainty, where the ensemble average might be calculated with equal contribution from each driving atmospheric model as a key factor that explains uncertainty[54,55] (Table S1). As modelled datasets, wave reanalyses/hindcasts are generally affected by methodological uncertainty factors, such as model resolution[56], forcing quality, parameterization[57] or downscaling methods[31], which can lead to discrepancies in the resulting wave climatology, especially in complex orographic areas around islands and in semi-enclosed seas (see right panels of Fig. 3(a), and Figs. S2-S7). The uncertainty of wave hindcasts is bound to be larger in enclosed and marginal seas than in open oceans due to the important role of the mesoscales and submesoscale dynamics[58]. Inter-product uncertainty increases for the extremes but it is still lower than the corresponding range of inter-annual variability (Figs. 3(a-b), S2, S3 and S6). The inter-product uncertainty of mean T_m (Figs. 3(c)) relative to the climatological value (Fig. S6) is similar to the H_s counterpart (after excluding an ensemble member that uses a different T_m formulation, see Table S1 and Fig. S4). There is a general agreement in large-scale θ_m features among products (Fig. 3(d) and S5).

Tropical cyclones (TC) tend to be underrepresented in reanalysis[59,60] due to their small-scale features, which affects the reliability of the resulting wave climate in the affected tropical areas. ERA5 underestimates TC intensities[61,62] despite having an atmospheric horizontal resolution of 0.25°(Table S1) that can potentially capture a realistic distribution of TCs[63]. As part of the Copernicus Marine Service, WAVERYS[64] was developed as the first global reanalysis with a fine resolution of 1/5°, and assimilation of wave directional spectra. Such high resolution makes this dataset an interesting source to study small-scale atmospheric features but the time period (1993 and onwards), together with the lack of ocean and atmospheric coupling, are limiting factors for the study of TC, as they are infrequent events sensitive to feedback processes[63].

Overall, wave reanalyses and hindcasts replicate coherent spatial global patterns of the main wave statistics, but special caution is needed in assessing trends as different models exhibit striking trend discrepancies[55,65–69] (Fig. 2(b) and S6-S7). This disagreement is arguably related to the presence of temporal inhomogeneities due to the increasing amount and type, as well as varying quality of observations assimilated over time[65,67,70]. Model accuracy potentially increases over time (reflected by a decrease in the inter-product uncertainty over time as illustrated in Fig. S9), which is not optimal for climate research and, in particular, trend assessment. For example, the number of observations assimilated in the ERA5 wave reanalysis[71] increased from approximately 0.75 million per day in 1979 to around 24 million per day by the end of 2018[72]. Additionally, temporal inhomogeneities are seen as more pronounced in the 90s and early 2000s (see Fig. S9), which relates to the assimilation of wave data from satellite altimeter missions starting in 1991 (Fig. 1), and the marked increase in the quantity of assimilated H_s, wind and surface pressure data in the following decade[65,72]. Trends calculated from CFSR[73]-derived wave products are markedly more negative than the other products (Fig. 2) because CFSR winds have a marked step change in 1994[69] (with a notable overestimation of winds before that) which coincides with the assimilation of new surface wind data[70,74]. Without considering CFSR-derived products the areas of robust signal increase (Fig. 2(b)).

Long-term century reanalysis products also have marked temporal inhomogeneities, with a notable difference in ingested data between the first and the second half of the 20th century[67]. Modelled data without assimilated observations presents value for trend analysis and signal detection and attribution[66,67,75,76] in that they are not affected by temporal inhomogeneities in employed observations. Furthermore, unconstricted models without data assimilation offer the possibility to generate Single Model Initial-condition Large Ensembles (SMILE), which can help investigate the internal climate variability and contribute to a more robust assessment of trends and low-frequency extremes[66,75].

Future wave climate

Since 1992, the IPCC has released sets of emission scenarios to be used for driving global climate models to develop climate change projections. These projections are usually carried out in the collaborative framework of the Coupled Model

Intercomparison Project (CMIP), which is developed in phases to foster climate model improvements and to support national and international assessments of climate change. The climate projections of the latest phase, CMIP6[77] (released in 2019) are based on the Shared Socio-economic Pathways (SSPs)[78], with focus on SSP1-1.9, SSP1-2.6, SSP2-4.5, SSP3-7.0, and SSP5-8.5.

However, most climate models do not provide information about waves (although there are a few exceptions[79]). To fill this gap, the impacts of global warming on ocean wind-wave characteristics have been explored by exploiting surface wind fields (and sea-level pressure) from global and high-resolution regional climate models as forcing for global and regional wave models (typically phase-averaged models based on the spectral action balance equation[2]), or as a statistical predictor to simulate wave fields[34]. While (physics-based) wave models can include complex wave interaction processes (for example, wave-ice interaction) and are able to reproduce mixed sea states better, statistical models have low computational cost and offer the advantage of flexibility in the choice of predictors (surface winds derived from climate models have typically low skill[80], and sea-level pressure gradients might be used instead as geostrophic wind proxies). Most of these wave modelling products provide only a few set of integrated wave parameters such as H_s, T_m and θ_m (see Box 1), having the impact of climate change on wave spectral parameters not been extensively studied yet[81,82].

The need to conduct a posteriori wind-wave simulations leads to limited availability of future wind-wave projections and, consequently, lower confidence of future changes in wind-waves in comparison with many other climate variables[27,39]. In addition, there is typically a delay between the release of climate projections from a CMIP phase and the corresponding derived wind-wave climates. While a few CMIP6-derived wave projections have been published already[79,83–85], most of the state-of-the-art published literature is still based on the CMIP5 phase[86] and the Representative Concentration Pathways (RCP) scenarios[86], with particular focus on the medium-stabilizing forcing scenario RCP4.5 and the high-emission scenario RCP8.5 (see Tables S2-S8).

Computational cost is an important factor for the generation of large ensembles[66], which are key to properly account for the main sources of uncertainty, namely, internal climate variability, climate model and wind-wave modelling approach, and forcing uncertainty derived from the greenhouse gas emission scenarios. Large ensembles over long enough time periods are also beneficial for a better characterization of extreme waves driven by rare but hazardous events, such as tropical cyclones (TC). However, most climate models have spatial resolution ranging from ∼250 km in the atmosphere to ∼100 km in the ocean, which cannot well capture TC genesis[87], intensity, frequency and variability, which makes the resulting global projections of extreme waves in TC regions uncertain[63]. Consequently, CMIP5[88] models have shown limitations in their ability to reliably represent inter-annual and inter-seasonal variability particularly within TC-affected regions[80]. Wave projections obtained with high resolution climate simulations (∼25 km or less) provide a more realistic overall distribution of TC-driven events[63,89,90] but there are still large uncertainties due to the lack of feedbacks, and errors in the wind fields[63]. The CMIP6 endorsed High Resolution Model Intercomparison Project (HighResMIP)[91], with a coordinated set of experiments with at least 50 km resolution in the atmosphere and 0.25° in the ocean, provides valuable climate data to better assess historical and future TC properties[87]. However, the existing wind-wave literature exploring such projections is still extremely limited[85,92].

The current knowledge of future projections of wave climate at a global scale was consolidated with the development and analysis of the first coherent, community-driven multi-method ensemble of historical and future global wave simulations[35–37], that resulted from a collaborative international effort in the framework of the COWCLIP project[28]. This CMIP5-driven large ensemble accounted for dominant sources of uncertainty[35] and has become a reference for the IPCC Special Report on the Ocean and Cryosphere[93] and IPCC AR6[39]. One important conclusion was that, generally, climate model-driven uncertainty dominates[35], which indicates the need for further model improvement. However, the internal climate variability was not properly sampled, and only two greenhouse emission scenarios were considered[35] (RCP4.5 and RCP8.5). Moreover, most global wave projections used to derive this large ensemble did not include the Arctic Ocean[94] despite being a hotspot for wave climate change with potential dramatic increases in wave energy due to sea ice decline[95,96]. The existing limited literature regarding CMIP6-derived wave projections[79,85,97] indicates better performance for the historical period when compared to ERA5[85]. Projected patterns of change obtained for SSP5-8.5 are similar to those obtained for RCP8.5[35,85]. However, more model combinations and further testing with more hindcast/reanalysis products are advisable to derive robust conclusions, considering uncertainties in contemporary[54] and future[35] H_s estimates.

At regional scale, the European-focused projects PRUDENCE[98] and ENSEMBLES[99], which ended in 2004 and 2009, respectively, where one of the first large-scale collaborative frameworks to develop regional projections to address the need for climate change information for use in impact and adaptation research. These initiatives were followed by the international Coordinated Regional Climate Downscaling Experiment (CORDEX) that provided the framework for downscaled CMIP5 datasets at resolutions ranging from 0.22° to 0.44°, which presents added value over the coarser resolution counterparts[100]. CORDEX CMIP6 atmospheric projections are expected to become available between 2023 and 2024 but, as for the previous CORDEX phase, wave information is not included. An additional shortcoming is that CORDEX domains are not tailored for ocean modelling research and, for example, do not cover several parts of the world oceans.

The first regional papers investigating the future wave climate mostly focused on the North Atlantic Ocean and the Mediterranean Sea (Fig. S10), in a similar fashion as for the historical wave climate. Despite the steady increase, the existing literature still unevenly covers the world oceans/seas without necessarily focusing on the coastal regions with most population on vulnerable land to coastal flooding (defined as land below the local high tide[101]) under present and future conditions[101] (Figure S11). Most of peer-reviewed regional scale literature is based on the RCPs (RCP4.5 and RCP8.5), and previous scenarios (A1B, B1, B2), with very limited CMIP6-derived regional projections[102–104] (Table S2-S5), and some of them assuming simplified boundary conditions[102].

In the late 2010s, news ways to present future projections and uncertainty were introduced. Climate projections have been assessed as a function of global warming above the preindustrial level, instead of using temporal and emission dependence. This perspective helps to investigate the benefits to limiting global warming, which became more relevant after the Paris Agreement of 2015[105] proposed to limit the increase in global warming to below 2.0° C, and preferably to 1.5°. However, this global warming level approach cannot be used with sea level rise projections as it does not correlate well with global mean temperature increase alone. There is very limited literature of projected changes in wave conditions as a function of warming levels[106] which can be explained by the limited amount of century-scale simulations of wave parameters that is needed to perform such an assessment. An alternative approach to represent uncertainty was introduced with the use of storylines[107] that are defined as physically-consistent and plausible future events or pathways that provide an actionable risk perspective. It is however a challenge to align this approach with the traditional model ensemble-based probabilistic approach, which might require changes in physical modeling to support the storyline approach[108]. This approach has, however, not been applied yet to assess the uncertainty of future wind-wave conditions.

Historical and future wind-waves by ocean basin

The impact of global warming on wind-waves varies across the global oceans. This section describes the historical and future wind-wave conditions for six major ocean basins: the Atlantic Ocean (including the Mediterranean Sea), the Pacific Ocean, the Indian Ocean, the Arctic Ocean, and the Southern Ocean. This review combines existing evidence from global to regional scale studies, and highlights the relative importance of the challenges introduced in the previous section. The description is articulated around four main aspects: climatology, historical trends, responses to large-scale teleconnection patterns, and future changes. Future projections focus on the changes by the end of century with the RCP8.5 scenario as this forms the largest body of state-of-the-art literature on wave climate changes. Whenever possible, changes are described for mean conditions, high-frequency extremes (90th to 99th annual percentiles) and low-frequency extremes (multi-decadal return periods).

The Atlantic Ocean (and the Mediterranean Sea)

Climatology

Visual and instrumental H_s observations acquired on weather ships operating in the North Atlantic Ocean from the late 1940s until the 1970s provided the first decadal records of mean annual H_s[40], which revealed a large variability across the whole Atlantic basin with inter-annual fluctuation of the same order as seen for the seasonal fluctuation[109]. Increasingly available wave records in the North Atlantic have enabled extended focused analysis in this region[110–113], showing a latitudinal gradient of the mean H_s and its inter-annual variability (Fig. 3(a)). Maximum H_s values have been recorded between Greenland and Europe (for example, the Quirin storm in February 2011 produced a H_s of 20.1 m[114], the largest recorded by satellite altimeter) and minimum values are exhibited in the Tropical Atlantic (Fig. 3(b)).

Due to a lack of in situ observations (Fig. 1), wave climate analyses in the South Atlantic are essentially based on model reanalyses[115] (Fig. 3) and satellite data[29,32] (Fig. S1). The South Atlantic annual mean H_s (and its inter-annual variability) also exhibits a poleward positive gradient (Fig. 3(a)) but the annual maximum H_s is lower than the North Atlantic Ocean counterpart (Fig. 3(b)). The annual mean T_m climatology is larger over the Southern Atlantic Ocean, and, particularly, over the Eastern side of the ocean basin due to the swell influence (Fig. 3(c)). In the extra-tropics, there is a mean westerly flow (waves coming from the west to the east) that rotates clockwise(anticlockwise) on the lower latitudes of the Northern(Southern) Atlantic Ocean, leading to the dominance of easterly waves over the Equator (Fig. 3(d)).

The Mediterranean Sea presents a more moderate wave climate, with complex spatial patterns associated with local circulation, complex orography, and fetch-limited conditions[116,117]. The highest recorded wind-waves in the Mediterranean are located in the Northwest Mediterranean Sea[118], where there is also the largest inter-annual variability[119]. For example, a record-breaking H_s of 8.44 m was observed by a buoy during Gloria storm in January 2020 off the Spanish coast[120].

Historical change

Annual mean and extreme H_s trends in the North Atlantic Ocean computed over decadal time periods mostly reflect the phasing with climate oscillations, with increasing and decreasing trends in the North East Atlantic over the 1950s-1990s[121–125] and 1990s-2020s[44,64] periods, respectively while North West Atlantic trends were positive over the 1990s-2020s[44,64]. The mean H_s

trends over the 1990-2020s lie within ± 1 cm/year but larger values in grid cells close to land and sea ice margins are exhibited by altimeter data[44,64]. For the 1950s-1990s period, observed trends range 0.5-3.4 cm/year for the mean H_s[125]. Several century scale H_s reconstructions based on atmospheric reanalysis indicate a general increase of the annual mean and extreme H_s over the 20th century[67,126] but these results are severely impaired due to the increasing number and changes in assimilated data[67]. Contemporary reanalysis/hindcast products show regional discrepancies for the North and Tropical Atlantic annual mean H_s trend over the 1980-2014 (Fig. 2(b))[127] but a robust increase is obtained for the summer mean H_s and high-frequency H_s in the Tropical Atlantic with regional averages of 0.5 cm/yr and 0.7 cm/yr, respectively[55]. Altimetry-based H_s winter trends over the North Atlantic Ocean starting 1993 are mostly caused by internal variability[128].

In the Southern Ocean, multi-decadal trends computed from altimeter data from the 1992-2018 period exhibit significant positive trends of the annual mean H_s in areas between 30-60°S (up to 3 cm/year) but discrepancies among satellite products are generally present in this basin[44] (Fig. 2). Contemporary reanalysis show a similar positive pattern for the annual mean H_s (but with lower trends, Fig. 2(b))[44], and an overall increase of the mean T_m during the austral winter exceeding 0.01 s/yr[55].

In the Mediteranean Sea, model reanalyses indicate an overall decrease of the annual mean H_s over the period 1958–2001[129]. Altimeter data and contemporary reanalysis indicate a significant increase in the western Mediterranean Sea after the early 1990s[44,119] (< 3 cm/yr) which is linked to increased winter extremes[119].

Response to teleconnections

The North Atlantic Oscillation (NAO) and Arctic Oscillation (AO) are leading modes of interannual North Atlantic wave climate variability[130], showing negative correlation with winter wave climate statistics (mean and extreme) in the southern North Atlantic and positive correlation northward of 50° N[52,131] (Fig. 4, Figs. S12-13). The East Atlantic (EA) and Scandinavian (SCAND) patterns are also relevant atmospheric modes for the North Atlantic Ocean[132], which govern winter wave activity towards more southern latitudes and contribute to larger wind-waves over the most western coasts of Europe during their positive phase (Fig. 4(a)). A negative phase of SCAND also contributes to larger H_s in the northern North Atlantic, including the North Sea (Fig. 4(b)). The Western Europe Pressure Anomaly (WEPA) has been shown to explain 40-60% of observed winter-averaged H_s (mean and extreme) variability off western Europe[133].

The Tropical and South Atlantic wave characteristics are poorly correlated to most climate variability patterns[134] (Fig. 4). However, the Atlantic Multidecadal Oscillation (AMO) is strongly correlated (at decadal time scales) to increased mean wave power within most South Atlantic regions[135]. Also, a 3000-year reconstruction of changes in predominant wave direction in a Brazilian coastal location (based on coastal morphology changes preserved in beach-foredune ridges) indicates that the Southern Annual Mode (SAM) is a primarly driver for multi-centennial cycles in θ_m[136].

In the Mediterranean Sea, the interannual variability of extreme waves in winter is dominated by the negative phase of the EA with a larger effect in the western basin (Fig. 4(b)). Additionally, a positive SCAND indicates larger(smaller) heights in the western(eastern) Mediterranean Sea[137] (Fig. 4(a)). The winter average H_s is also anti-correlated with the winter NAO[129]. However, while large scale patterns influence the Mediterranean wave field, the wave dynamics in the Mediterranean are strongly influenced by the regional orographic conformation and fetch, which acts as filter to favor atmospheric circulation components that are more effective in producing waves due to the basin configuration[129].

Future projections

There is strong consensus towards decreasing mean H_s (0-10%) (Fig. 5), T_m (0-5%) and wave energy (0-5%) across much of the North Atlantic[35,138,139] (Figs. 5 and S14-15). This decrease is statistically significant for both RCP4.5 and RCP8.5 but it is more intensified for the latter (up to ∼5% vs. up to ∼10% H_s change for the low and high emission scenarios, respectively)[35]. High-frequency H_s extremes are (overall) projected to decrease (0-10%), but such changes are not robust amongst models and assessments[140]. Multi-model ensemble projections of 100-year return period H_s[140] exhibit a projected increase for sub-arctic regions and the South Atlantic Ocean (0-20%), where there is also a projected increase in energy flux >10%[141,142].

θ_m is projected to shift clockwise (up to 10 degrees) for most North Atlantic areas and anticlockwise (up to 10 degrees) for high-latitude areas (>50° N). These changes are consistent with a projected decrease in future mid-latitude storm activity, driven by a projected northward shift of North Atlantic storm tracks to higher latitudes, on top of more frequent atmospheric blockings[138]. The projected signal of change in wave characteristics for the tropical Atlantic regions is uncertain[34,35] (Fig. 5), except for θ_m, which shows a consistent clockwise rotation of up to 10 degrees. In the South Atlantic, small projected future increases in extreme H_s and T_m values have been obtained but they are not consistent amongst models and assessments[34,35].

Projections using high-resolution atmospheric forcing fields (with a better representation of hurricane events) show that the annual maximum H_s is projected to decrease off North America but increase (up to 0.5-1 m) along South America and North Europe's Atlantic coast under RCP8.5[89]. However, the projected 20-year return period of H_s varies widely along North America's Atlantic coast and the Gulf of Mexico and highly depends on forcing resolution[63]. CORDEX-based single-model simulations downscalled along the European coastlines show decrease in the mean H_s (∼ 10%) but (a less robust) increase (∼1 m) in the annual maxima resulting from a widening of the probability distribution[143].

In the Mediterranean Sea, global and regional future projections show a general decreasing trend in mean H_s (0-10%), T_m (0-5%) and wave energy[35,144–146] (Fig. 5), with a slight eastward shift in θ_m[144] and an increase in multimodal wave climate[146]. However, in some localized energetic areas, such as the Northwestern Mediterranean, mean and extreme waves might increase[147]. For example, a multi-model assessment of the H_s associated to Mediterranean Hurricanes shows that their 100-year return period is projected to increase around Balearic Islands and Sicily (<10%)[148].

The Pacific Ocean

Climatology

The Pacific Ocean historical wave climatology and its relevant extreme statistics have been described using multi-decadal model hindcasts or reanalyses[68,149] complemented by satellite altimeter-based records[150], ship observations[151], and regionally focused buoy data assessments[45,110,152,153]. Within mid to high-latitude areas (>45° N and <45° S), there is a well-documented unimodal wave climate[154] driven predominantly by Northern and Southern Hemisphere mid-latitude storm systems with temporally-averaged wave energy and H_s reaching their peaks. The largest annual mean H_s occurs in the mid-latitudes of the Southern Hemisphere, while the annual maxima takes place in the Northern Pacific Ocean, exhibiting a similar latitudinal gradient as the Atlantic Ocean (Fig. 3). For example, the strongest storms in the Eastern North Pacific have generated H_s in the range of 14-15 m[153].

The North and South Pacific extra-tropical areas show large seasonality and inter-annual variability (Fig. 3). Within equatorial tropical regions (>30° S to <30° N), a complex multi-modal wave climate prevails almost everywhere (driven by remotely-generated swells and higher-frequency waves generated by prevailing trade winds)[154] and temporally-averaged wave energy and H_s exhibit relatively lower values. The Southern Ocean generated swell is a dominant influence, particularly in the south-east Pacific Ocean, where the annual mean T_m largely exceeds 10 s (Fig. 3(c)). The Pacific islands possess a wave energy resource of high interest to wave energy developers, owing to its high power and low variability[9].

Historical change

Satellite altimeter data shows that North Pacific displays statistically significant negative trends in the annual mean H_s (< 1 cm/year) between 1985-2018 (Fig. S1), despite mean wind speed showing no clear trends across these basins[32,44]. Similar negative trends are also obtained in parts of the North Pacific Ocean by some contemporary reanalysis/hindcast products for 1980-2014 (Fig. 2). In the sub-tropics, contemporary reanalysis/hindcast products show a clockwise rotation of θ_m during winter season. Following adjustments to correct for inhomogeneities in buoy records, slightly positive significant trends in mean H_s are observed off North California and negative trends off Alaska and British Columbia but no significant trends were found in extreme H_s[45]. In the western North Pacific, the observed wave energy by buoys increased significantly on the Pacific side of eastern Japan over the period 1980-2009, in agreement with modern reanalysis[155] (Fig. 2). Altimeter-derived trends exhibit non-significant positive values for high-frequency extremes, such us the 90^{th} percentile, for specific northern regions (>1cm/year) and gradually become more negative further south (-0.3 cm/year). For 1991-2015, satellite data shows consistent H_s increases (0.56 cm/year and 1.25 cm/year for the mean and 99^{th} percentile, respectively) in the Northwest Pacific and Japan Sea[156]. However, these extreme Hs trends can be affected by the undersampling impact on altimeter derived trends[47].

A regional reconstruction of H_s between 1911-2010 shows that seasonal maximum values appear to have increased during summer and spring over the central South China Sea and during summer for the East China Sea (>2cm/year), although trends are predominantly negative across both regions[157]. No trends in mean H_s are observed in the tropical Pacific[32,44] for either mean or high frequency H_s extremes over the periods 1985-2018 and 1992-2017, with modern reanalysis showing inconclusive results there[44] (Fig. 2).

In the South Pacific, the altimeter record shows no clear trend for the annual mean H_s over 1985-2018 except in the Southwest Pacific, where trends are statistically significant negative (<1 cm/s, see Fig. S1), whereas there is a significant positive trend (0.5-1 cm/year) for high-frequency H_s extremes (90^{th} percentile)[158]. Conversely, wave reanalysis/hindcast show a consistent increase in the annual mean H_s over the Southern Ocean that exceeds 1 cm/s (except for CFSR-derived products) (Fig. 2), which relates with an increase in the mean and high-frequency H_s extremes during the austral winter[55]. Analysis of buoy records along Australia's east coast display small significant positive trends in the north (Coral sea coast), and small significant negative trends in the south (Tasman Sea coast) (with absolute magnitudes <0.5cm/year)[159].

Response to teleconnections

The Pacific Ocean region is strongly influenced by recurring patterns of atmosphere-ocean climate variability which force anomalous atmospheric and ocean wind-wave characteristics at inter-annual to multi-decadal time-scales[160]. The El Niño Southern Oscillation (or ENSO) is a key pattern of Pacific inter-annual climate variability, with its extreme phases (El Niño and La Niña events) strongly linked to anomalous spatial and temporal wind-wave characteristics[16]. The Southern Oscillation Index (SOI) gives an indication of the development and intensity of El Niño (negative values of the SOI) or La Niña events (positive values of the SOI) in the Pacific Ocean. CMIP5 models can on average capture the major observed mean and extreme H_s

responses to ENSO[161]. Satellite altimeter-based records and model data show that El Niño events are associated with elevated wave energy levels and increased H_s over the south-west tropical and Northeast Pacific regions (see Fig. 4(b)), and reduced wave energy within Northwest Pacific regions[14,51,142,161,162]. In contrast, La Niña phase events have been linked to elevated wave energy levels and H_s values for most South and Northwest Pacific regions[51,162]. The ENSO also affects θ_m with El Niño events forcing anticlockwise (southerly) /clockwise (southerly) rotations across Northeast / Southwest Pacific regions[14,162].

Extreme Pacific Decadal Oscillation (PDO) phase events lead to similar spatial patterns on multi-decadal time-scales but reduced wave energy flux anomalies relative to ENSO events[162]. High wave intensity is experienced over most Northeast Pacific regions during PDO warm (positive) phase (see Fig. 4(a)) and decreased wave intensity is more common during PDO cool (negative) phase[162]. The Pacific-South American and Pacific-North American (PNA) modes have also been correlated with South and North Pacific Ocean swell waves generated, respectively, that travel equatorward[53]. Significant increases in extreme H_s over central North Pacific areas are found to be connected with a deeper and eastward extended Aleutian low[44].

Future projections

Across the North Pacific, tropical Northwest Pacific and extra-tropical South Pacific regions, global scale projections exhibit a strong agreement that annual and seasonal mean H_s will decrease (5-10%) by 2100 under RCP8.5[35] (see Figs. 5 and S14). This decrease relates to a decreased north-south pressure gradient and wind speed[35,163]. Single-model regional projections over the East China Sea show similar projected decreases for the mean H_s but wind-sea dominant H_s high-frequency extremes are projected to increase (>10% in summer), which are likely related to projected changes in the local winds[164]. Fewer large wave events are also projected for eastern Australia (-42% for RCP8.5)[165]. In contrast, tropical East Pacific areas exhibit robust positive projected changes for annual mean H_s (up to 5% for RCP8.5 and up to 3% for RCP4.5) and annual number of high-frequency wave storms (up to about 25-50%)[37]. Robust increases in 10-year return H_s up to 15% are also seen in the tropical Pacific for a 3°C warming level (which occurs in the range of years from mid to the end of the century for RCP8.5 scenario)[106]. This projected increase in H_s is mainly attributed to the projected increase in southeasterly Pacific trades[33,166] and is associated with an El Niño-like mean circulation intensification[106]. Analysis of projected change in the spectral characteristics indicates the swell energy from the Southern Ocean is also a major contributor to this increase[82].

In terms of typhoon-driven extreme H_s (with a probability of occurring once every ten years), wave ensemble projections show changes ranging 30% for Northwest Pacific regions (positive changes around Japan and negative changes for Southeast China Sea regions) owing to a future eastward shift of typhoon tracks[89]. However, these estimates are affected by large uncertainty levels associated with typhoon intensity and track projections. There is also uncertainty regarding how TC-driven waves will change around Pacific Islands as different projections exhibit a large range of possible variations[167]. Projections in the upper tail of the H_s distribution are unclear nearly everywhere[34,35], yet ensemble projections of 20-year[166] and 100-year return period H_s[140,168] show a projected increase for sub-arctic regions (5-10%) and a projected decrease across South and tropical Northwest Pacific regions (5-10%).

In terms of the annual mean T_m, there is a projected decline for Northwest and Southwest Pacific areas (up to 5%) and a projected positive change for East Pacific regions (up to 5%)[35,168] (Fig. S15). An extended energy increment of <10% (for 100-year energy flux) is projected throughout the subequatorial-tropical and north-eastern Pacific Ocean partly due to increased swell influence[142]. Mean θ_m are projected to change clockwise over sub-tropical and tropical regions and anti-clockwise at high-latitudes (5°-10°)[35].

The Indian Ocean

Climatology

Historical climatology in mean and extreme H_s have been analysed based on ship-reported wave data[169,170], in-situ buoy data[169,171,172], hindcasts[173–177], reanalyses[65,178–180], and satellite altimeter data[32,44,181–183]. As exhibited in other basins, a poleward positive gradient in mean H_s and its interannual variability is found across the Indian Ocean (Fig. 3(a)). The Indian Peninsula/subcontinent divides the North Indian Ocean (0-30°N) into two basins: the Arabian Sea to the west, and the Bay of Bengal to the east. The dominant feature of the North Indian Ocean is the monsoon winds, which reverse direction annually and are an example of intense ocean-atmosphere interaction at basin scales[184].

In the South Indian Ocean, the extratropical westerly winds dominate. Strong seasonal signals are observed in both mean and extreme H_s year-round, with a peak during June-August[14,185]. The Southern Ocean swell is a dominant influence, that propagates northwards across the basin to impact on the coasts of the Indian Peninsula/sub-continent (and islands)[14] (Fig. 3(c)). For example, in May 2007 southern swell that originated around 40° S impacted Reunion Island with $H_s > 6$ m, as recorded by altimeter data. The climatological mean value of T_m presents high values in the entire domain except the eastern Arabian Sea, where wind sea states are more dominant[183,186–188] (Fig. 3(c)). Like the Pacific islands, the islands in the South Indian Ocean are locations of interest in relation to their potential for wave energy extraction[9].

Historical changes

Contemporary hindcasts/reanalysis products (without considering CFSR-derived products) agree in a robust positive mean and extreme (90^{th} percentile) H_s trend for a large fraction of the Indian Ocean over 1985–2015 for the months of December to February (with an average of ∼0.4 cm/year and ∼0.6 cm/year, respectively, over the areas of positive increase)[55]. Modeled data also shows a mean T_m increase during winter in the Southern Indian Ocean[55]. The seasonal H_s increase is reflected in a positive annual mean trend[127] in the Southern Indian Ocean with a rate <0.4 cm/year (Fig. 2). Different altimeter data products show conflicting signals over latitudes north of 30° S for the period 1992-2017[44]. Available merged altimeter H_s data for the 1985-2018 indicates non-significant trends for both mean and high-frequency extremes north of of 30° S, while a large area with positive trend (>1 cm/yr) is depicted south of 30° S[32].

Seasonal analysis of individual wave reanalysis depict a large increase in H_s (∼1.2 cm/yr) over the North Indian Ocean during the summer monsoon period as compared to other seasons[183,185,186]. Single product assessments also exhibit declining regional trends of the 90^{th} percentile winds in the Arabian Sea[180] and increasing trends in the central Bay of Bengal[176] for the period 1979-2012, with corresponding influence on the locally generated sea (0.2 cm/year). However, an ensemble of contemporary hindcasts/reanalyzes shows little changes for the North Indian Ocean H_s statistics[55].

Response to teleconnection patterns

Natural climate variability such as ENSO, the Indian Ocean Dipole (IOD), and the Southern Annular Mode (SAM) exert significant impacts on wind and wave climate over the Indian Ocean[51,118,185,188–191]. In the summer monsoon, El Niño amplifies the tropical cyclone activities in the Bay of Bengal leading to a significant increase in H_s there[185,192]. In contrast, in December to February, El Niño weakens the tropical Walker cell and trade winds and thus reduces H_s over the Tropical Indian Ocean[161,193,194]. Monsoon-driven winds and Boreal Summer Intra-Seasonal Oscillation (BSISO) modulate the wave activities in the Tropical Indian Ocean during the summer monsoon[195]. The positive IOD events decrease H_s in the Arabian Sea due to the change in the direction of wind patterns during September-November[185,196]. Further, the SAM being a dominant mode of the Southern ocean not only affects the wave climate over the Southern Indian Ocean but also drives changes over the North and Tropical Indian Oceans year-round[185]. Intra-seasonal variation of surface zonal wind induced by the Madden Julian Oscillation (MJO), that traverses eastward from the western tropical Indian Ocean to the eastern tropical Pacific, is associated with anomalies in H_s, T_p and wave energy flux[197].

Future projections

The projected wind-wave climate in the Indian ocean has been assessed from both global and regional studies[34,94,198,199]. Seasonal mean and high-frequency extreme H_s increases up to 10% and 20%, respectively, are projected over areas of the North Indian Ocean during all seasons other than December to February, and over the western Tropical Indian Ocean during the months from June to November in line with the projected circulation change towards an IOD positive phase-like mean state[161] (under the RCP8.5 scenario). Winter mean H_s exhibit a robust decrease over the western Indian Ocean from 30°N to 30°S (up to 10%)[35]. However, areas of statistically significant increases (<20%) of 100-year return levels are projected[140]. The annual mean T_m shows robust increases in the North Indian Ocean (<5%) (Fig. S15) due to an increase of the Southern Ocean swells[35,81], as well as a counterclokwise rotation in the western side of the basin (up to 5°)[35].

The Southern Indian Ocean displays relatively consistent signals of projected change of the mean H_s, with increases in high-latitudes and decreases in mid-latitudes (<5% for RCP8.5) throughout the year (see Fig 5), which is related to future change in SAM toward its positive phase[161]. 20-year return period are projected to increase in the high-latitudes and eastern mid-latitudes[140], which also increased mean T_m due to increased southern swell influence[81]. Additionally, the assessment of changes in spectral characteristics[81], with emphasis on the extremes[200], shows zones of projected decrease in annual mean H_s in the southeast Indian Ocean, associated with the projected future southward shift in westerly winds in the region[201].

On a regional scale, future projections of wind-wave climate have been assessed mainly in the North Indian Ocean. Along the Indian coasts, annual mean H_s has been projected to increase by up to 30%, and wave periods of 20% and 10% on the east and west coast, respectively[180]. On the west coast, 100-yr return periods H_s have been projected to increase between 5 and 58%[202]. Projected increases in H_s of 5% around Reunion island have been suggested, associated with a 6.5% increase in the intensity of cyclones in the region[203]. In the Persian Gulf, a future decrease in wave power (up to 40% in the northern Persian Gulf) is projected[203], with both H_s and T_p decreasing approximately 15% and 5%, respectively, for all scenarios[203,204]. Conversely, CMIP6-based projections indicate an increase of 21 to 45% in the Gulf of Oman future's wave power under SSP-5.8.5[104]. Along the Indian Ocean coast of Australia, the projected increase and anticlockwise rotated offshore wave conditions have been propagated onto the coast[205]. Nearshore, the influence of future sea-level rise (SLR) on the nearshore transformations of wave climate were found to dominate any effects of projected changes in offshore wave climate on the future incident wave climate.

The Arctic Ocean

Climatology

The Arctic Ocean is characterized by several semi-enclosed seas such as the Barents, Kara, Laptev, East Siberia, Chukchi, and Beaufort. The largest waves occur in the Norwegian and Greenland Seas as a result of extratropical cyclones that can travel from the North Atlantic to the Barents Sea[206]. Atlantic waves also propagate northwards into the Baffin Bay Davis Strait corridor, where they typically encounter wind-sea states traveling in opposite directions[207,208]. The influence of waves from the Pacific on the Arctic wave climate is minimal, as the two basins are connected only by the narrow Bering Strait.

In the Arctic Ocean, wave fetch greatly depends on sea-ice extent and complex wave-ice interactions take place in the marginal ice zone, such as ice-induced wave attenuation and scattering[209,210]. Sea ice has historically reached its minimum and maximum extents in September and March, respectively[211]. Seasonal sea ice forms in early to late fall, and subsequently breaks up sometime in late spring or early summer. This sea ice cover fluctuation leads to a large H_s seasonal cycle, particularly in the Baffin Bay, Beaufort-Chukchi, East Siberia, Laptev, and Kara Seas[207], where wave generation has been mostly occurring during the summer season. The wave season is, however, expanding as a result of sea ice retreat. For example, an unprecedented H_s of 5 m was measured by a buoy in the Beaufort Sea in October 2015 for the first time[3,212].

Historical changes

The historically limited influence of wind-waves in the Arctic region, in combination with the lack of in-situ observations and complex wave-ice interaction processes, has led to very limited studies about the Arctic Ocean wave climate until the 2010s. The Arctic Ocean wave climate has gradually received increased attention as a result of Arctic sea ice extents reaching unprecedented minima in 2012 and 2020[213], coinciding with longer records of available altimeter data[214]. The resulting increase in fetch has resulted in enhanced sea states and the emergence of swell energy notwithstanding any changes in wind magnitude, direction, and duration[3,207].

Both hindcast data[68,214–216] and altimeter observations[207,214,217] show increasing wave energy across all Arctic, with an upward trend of 1-3 cm/year for the mean H_s during 1990s to 2010s, and up to 10 cm/year for high-frequency extremes (99^{th} percentile). In particular there are wide spread increases in autumn waves, with trend strengthening in 1990s-2010s in comparison to 1980s-2010s[215,216]. Such an increase in H_s cannot be explained by wind speed alone[215,218], although there is a strong correlation between H_s and wind speed[214,219]. It is, however, difficult to quantify the isolated contribution of the wind speed on wave growth due to existing feedback mechanisms between wind and sea ice.

In the Atlantic side of the Arctic that is less affected by changes in seasonal sea ice, the Norwegian Sea exhibit decreasing trends in the mean H_s ($\sim$1 cm/year), which can be explained by a decrease in wind speed[207]. High-frequency H_s extremes there seem to have increased and decreased during, respectively, spring and fall ($\sim$1 cm/year) but with regional discrepancies among contemporary reanalyses/hindcasts.[68]. Merged altimeter data shows a significant negative trend for the mean H_s in the Nordic Greenland Sea ($\sim$1 cm/year), which can be explained by a decrease in wind speed[207].

Response to teleconnection patterns

The AO and NAO are correlated with the Norwegian and Greenland H_s[131,206,207], with their positive phase contributing to larger waves there (see Fig. 4(a)). The decreasing trend in NAO is expected to have caused the decreasing trend in the wave extremes of the Atlantic side of the Arctic that is not affected by sea ice[207,220] . PDO is negatively correlated with mean and extreme H_s in the Barents Sea over the last two decades (1992-2014)[207,217]. Differently, a weak positive correlation is found between PDO and the Beaufort-Chukchi Seas, which is arguably caused by the strengthened Easterly winds when PDO transitions into a positive phase that flow parallel to the ice edge in this region[207].

In the inner Arctic, historical observations and future projections seem to indicate a weakening of the Beaufort High, which seems to relate to a pan-Arctic intrusion of North Atlantic cyclones favoured by sea ice retreat[221]. In 2017, an intrusion of low-pressure systems from the North Atlantic, along the East Siberian coast, into the Arctic basin, produced a collapse of the Beaufort High, which featured an anomalous reversal of the normally anticyclonic surface winds and sea ice motion in the western Arctic[221].

Future projections

It has become evident that the Arctic is a hot spot for global climate change. Climate warming is amplified in this region, with air temperatures rising at least three times as fast as the global mean[222,223]. Sea-ice loss is a key driver of this enhanced Arctic warming, driving positive feedback, or so-called Arctic Amplification[224]. In addition, there is growing evidence that waves can contribute to this positive feedback mechanism by means of sea ice breaking and melting[209,212,225], but this has not been properly quantified to date.

The reduction of sea-ice extent and lengthening of the open water season, together with changes in surface winds, leads to projected increases in waves much larger than any other region of the world exceeding 50% regionally and 400% locally under RCP8.5 (Fig. 5 and S14-15). Average winds over the Arctic Ocean are projected to strengthen locally by up to 50 % during the fall and winter seasons and with the frequency of extreme winds speeds doubling in some areas[226]. The Arctic will be virtually ice-free in September by 2050 independent of the emissions scenario[227]. By 2100, these combined effects result in projected widespread monthly H_s increases above 70° N from July to November, with the annual maxima occurring later in the year (for example, shifting from September to November in the Beaufort Sea)[95,96]. A counterclockwise rotation of θ_m in the Beaufort Sea might indicate a weakening of the Beaufort High. Projections of the annual maximum H_s amount up to two to three-fold increase along some coasts and up to 6 m offshore in the Arctic Ocean and Greenland Sea under the RCP8.5 scenario[95]. While changes in winds are an important driver, they alone cannot explain the projected increases in the largest waves, as similarly observed for the historical period[95].

Overall, projected increases in Arctic waves are statistically robust. However, uncertainty in the specific estimates arises from the lack of a large ensemble of Arctic wave projections that can properly cover the large inter-model and inter-scenario variability in the Arctic region—there are just a few regional assessments and most of global projections do not include the entire Arctic Ocean[94]. Upcoming CMIP6-based Arctic wave projections might present lower uncertainties as CMIP6 sea ice extent projections have a lower inter-model spread with more realistic estimates in comparison to the CMIP5 counterpart[227,228]. However, the ocean wave modelling approach presents a notable source of uncertainty in this region due to the scarcity of data, the complexity of sea ice-wave interactions, and the consequent sensitivity of wave simulations to different sea ice parameterizations[95,212,229].

The Southern Ocean

Climatology

The Southern Ocean is defined here as the region between 40°S and 60°S, south of the continents of Australia, Africa and South America. It is unique, in that it represents a continuous body of water encircling the Earth with the only significant spatial constraints being the 1000 km wide Drake Passage between South America and the Antarctic Peninsula, and the seasonal advance and retreat of the Antarctic sea-ice extent[230]. The consequent long fetches, combined with continuous progression of low-pressure systems which propagate across the Southern Ocean, mean that, in addition to a sustained year-round intense wave climate, the region is also the generation source for swells influencing the wave climate of the Pacific, Atlantic, and Indian Oceans[158] (see Fig. 3(c,d)). Priority areas for wave power extraction have been identified over the southern hemisphere, including coastlines of New Zealand, Australia, and south of Africa.[9]. Decadal variability of associated wave power follows that of the change in swell wave height[9].

Due to the remoteness of the Southern Ocean, there are few in-situ buoy assessments of wave climate[14,158,231,232] (Fig. 1). Global model datasets combined with satellite data are needed to characterize the Southern Ocean wave climate[32,44,150,186,187,233,234]. The long uninterrupted fetches and sustained year-round strong westerly winds of the Southern Ocean lead to an annual mean H_s higher than any other ocean basin[183,234] (Fig. 3(a)). However, relative to similar latitudes in the North Atlantic and North Pacific, extreme wave conditions are lower[67,187,235] (see Fig. 3(b)) and seasonal variation is relatively small. While the Southern Ocean wave climate is spatially quite homogeneous with a band of high waves encircling the Earth at approximately 50°S, wave conditions are highest between Africa and Australia, and lowest to the east of the constricted Drake Passage (Fig. 3(a)). The maximum recorded H_s by in-situ buoys is 12.5 m, recorded in April 2012 south of Australia, but individual waves close to 30 m might occur[158].

Historical changes

Model datasets[67,127] (except CFSR-derived products) and altimeter data (Figs. 3(a), S1 and S7) show broad regions of significant increasing mean H_s across the Southern Ocean ranging 1-3 cm/year over 1980s to 2010s[32,186], with intensified rates for the Southern Ocean Atlantic Section over 1992-2017[44]. This increase is associated with strengthening of the westerly winds and a migration of the low-pressure systems to higher latitudes[236].

Changes in extreme wave conditions are less well understood due to limitations in both altimeter and model datasets under extreme conditions, and the scarcity of in-situ observations[158]. The limited data does, however, suggest an increase in the frequency and intensity of storm peaks, leading to a larger increase in Southern Ocean extremes than mean conditions[14,32,186,231,232,235], with larger extensions of positive increase exhibited for the austral summer[55].

Response to teleconnection patterns

The key mode of interannual wave climate variability in the Southern Ocean corresponds with the SAM[14,51,53,190], which is a dominant mode of atmospheric variability in the Southern Hemisphere[237,238]. The latitudinal shift in Southern Hemisphere mid-latitude westerlies moves polewards/equatorwards in its positive/negative phase[239], and influences the spatio-temporal characteristics of the wave field. During the positive SAM, the stronger zonal wind over the unobstructed Southern Ocean leads to larger waves there (Fig. 4(a)), which propagate northwards and might cause positive anomalies of the T_m in the Pacific Ocean[190]. The signature of the SAM in wind-waves thus extends beyond local wind-generated forcing in the Southern Ocean, and can affect the Northern Hemisphere extratropics, especially for the years that are not influenced by El Niño[190]. The

Pacific-South American modes are another important influence on the Southern Ocean wave climate, with the PSA-1 mode being positively correlated with H_s variability in the southeast Pacific and negatively correlated in the Indian Ocean sector of the Southern Ocean[53].

Future projections

Existing studies show consistent projected increases in the Southern Ocean wave climate, with the rate of increase larger for the RCP8.5 scenario than for RCP4.5[37]. These projections show increases in annual mean H_s by 2100 under RCP8.5 of approximately 5% (Fig 5). There is also an increase in the annual T_m (3%) (Fig. S15) and a counterclockwise rotation of the θ_m of approximately 3° to 5°. Similar ensemble projections of low-frequency extreme wave conditions[67] show a projected increase in 100-year return period H_s of approximately 7% for RCP8.5. Like in the tropical Pacific Ocean, there are also robust increases in 10-year return period H_s up to 15% (∼1m) over the Southern Hemisphere high latitudes by the end of the century, particularly at 3°C warming. These increases are associated with an increase of the SAM positive phase[37,106]. Regarding high-frequency extremes, global projections show a robust increase in the frequency and intensity of storms[37].

CMIP6-based single-model regional projections over the Bass Strait and south-east Australia agree to project an increase of the mean H_s (7%) in the offshore regions but reveal a decrease (2%-3%) in some nearshore areas due to decreases in the local wind[103]. This highlights the importance of accounting for local atmospheric and morphological conditions in assessing nearshore wave climate changes. As in the Arctic ocean, existing literature of future Southern Ocean wave projections at both global to regional scales consider simplified sea ice-wave parametrization without sea ice coupling. Wind-waves can have an important role in sea ice break up and sea ice retreat[209], meaning current projections of sea ice retreat and H_s increase near the Antartica could be underestimated.

Regional impacts of wave climate change

The potential wave climate changes in a warmer world can in turn impact coastal communities and marine-built infrastructure. A comprehensive review of the physical impacts of changes in wave action is out of the scope of this paper but here we provide some examples that illustrate how wave climate change might exacerbate coastal vulnerability.

Coastal damage in the Atlantic coast of Europe

During winter 2013/14, the Atlantic coast of Europe faced the most energetic and persistent extreme wave conditions of the last 67 years[240], and many coastal damages were reported. Some of the few existing long-term beach surveys revealed unprecedented sediment loss[240,241], and permanent coastal change occurred along rocky coasts, with some coastal cliffs experiencing retreat rates 2 orders of magnitude greater than the long-term average[242]. Despite the large impacts, the observed wave extremes have been mainly explained by the natural variability of the climate system[113,125,243] and it is still under debate whether future extreme wave conditions over Western Europe will be more or less frequent and/or intense. Yet, current knowledge of the wave climate indicates that periods of intense wave activity will continue to occur during the 21st century, and the combined impact of extreme wave conditions with increased SLR represents a major threat for densely urbanized coastal zone[244].

Flooding and erosion in the Pacific and Indian coastlines

Wave climatological variability associated with El Niño, along with contributions from storm surges and seasonal sea-level anomalies has been observed to be key control of coastal vulnerability for all land masses bordering the Pacific[16,162,245]. Extreme coastal response on the US Pacific margin has been observed with El-Niño-driven anomalies in winter wave energy and direction[16]. Anomalous wave directions have also been linked to extreme coastal erosion in South East Australia[17] Also, storm wave-driven flooding events across the Pacific atolls have been linked with remotely generated swells from the North Pacific[246], and most Pacific Ocean atolls will be uninhabitable by 2050 due to sea level rise exacerbating wave-driven flooding[247]. The Maldives in the Indian Ocean is similarly subject to wave-driven flooding, and flooding will become increasingly common in the region as sea levels continue to rise[248–250].

Impact on coastal and offshore structure design requirements

Wave climate change might impact coastal and offshore structure design requirements worldwide. In addition to sea-level rise, it is important to estimate future long-term changes in extreme water levels caused by storm surges, and wave height for coastal hazard mitigation[251]. For example, TC intensity is expected to increase in the mid-latitudes of the Northern Pacific[251], and associated future projected wave height increases dictate an increase of up to 1.5 m in breakwater caisson width of a typical in Japan[252,253]. Similarly, a change in the design of offshore wind turbines located along the west coast of India is required to avoid a decrease in fatigue life caused by the impacts of wave climate change[254].

Increasingly vulnerable Arctic coastal communities

Vulnerable Arctic coastlines have traditionally been protected from marine drivers by the presence of year-round sea ice. The frequency of extreme water levels and erosion events are anticipated to rise due to the combined action of waves, rising sea levels, storm surges, tides, and intensifying permafrost degradation[255,256]. This combined action has a dramatic impact on the Arctic coastal ecosystems and communities, exacerbating existing vulnerability of Indigenous communities located in low-lying coastal areas[95]. Wave storms (for example, Fig. S15) have already caused flooding and infrastructure damage. The decreasing distance between the ocean and the coastal settlements continues to threaten homes, water resources, infrastructure, and sites of historical and cultural significance[257–259].

Robust change in the Southern Ocean with unclear impacts

The Southern Ocean exhibits some of the more robust evidence for both historical and projected future change[32,35], yet the regional impacts of this change are still poorly known. Other marine drivers can exacerbate or compensate wave-driven changes. For example, climate-driven changes in waves impacting Australia's south-west coast might be more affected by SLR modulating the coastal wave field, as opposed to changes in the southern ocean wave field[205]. The implications on the Antarctic coast are unclear owing to the complexity of interactions but wave-induced flexure of the outermost ice shelf regions has been deemed a factor in ice sheet disintegration events along the Antarctic coast over the 2010s[230].

Summary and future perspectives

The climatological variability and change in wind-wave characteristics (see summary of key features in Table 1) have increasingly gained attention in recent years, with recognition of the potential impacts such changes can have on coastal systems, and design requirements for coastal and offshore infrastructure. These impacts could exacerbate, and in some instances exceed, the impacts of sea-level rise (SLR). There are several regions of the global oceans where these changes, and their consequent impacts, are already experienced. However, monitoring of wave climate change is limited by available observation systems. Historical change assessments to date are primarily based on satellite altimeter data (limited to estimates of significant wave height, and statistics affected by undersampling issues), in-situ buoys (sparsely distributed, and incomplete records of technology changes through the record have hampered trend investigations), and visual observations (limited accuracy and sampling and observational biases).

Wave reanalysis and hindcast products are often used as observation proxies due to the spatial and temporal scarcity of observations, but they suffer from temporal inhomogeneities as a result of the changes in quantity and quality of ingested observations, which can particularly affect trends. Despite these challenges, there is a general agreement of a consistent historical increase in mean wave heights over the Southern Hemisphere. There is also evidence of atmospheric teleconnection patterns having a strong influence on wind-wave variability. Future wave climate projection studies have primarily focused on mid (RCP4.5) and high (RCP8.5) emission scenarios on ice-free areas, showing statistically significant increases in the mean wave heights over the eastern tropical South Pacific and the Southern Ocean, and decreases over the North Hemisphere. Differences between 1.5°C and 2°C worlds reveal potential benefits of limiting global warming over large regions of global ocean. However, there is a large uncertainty among different climate and wave modelling approaches which particularly affect extremes for which studies show inconclusive results. Moreover, there is limited knowledge of how the ocean wave climate variability, and the interaction of waves with other marine and atmospheric drivers (sea ice, storm surge, sea level rise, coastal morphology change, surface winds, etc.) might affect wave climate change estimates. Limited studies of the Arctic Ocean show outstanding changes there due to sea ice decline but this needs to be further assessed with larger ensembles with improved climate forcing and better sea ice parameterizations. With the recognition of the present challenges, we discuss priorities for future research.

Sustained increase of observations

The emerging availability of new satellite sensors able to resolve a more complete picture of the wave field (such as SAR missions and CFOSAT SWIM sensors[43,70], which provide directional wave information), low-cost buoy sensors, and increasingly open access to previously private data holdings will provide greater opportunity to monitor wave field changes. For example, the SOFAR spotter network exceeded 600 buoys in March 2022 and continues to expand rapidly providing a rapid increase in global coverage of wave measurements[260]. However, it is equally important to invest resources in sustaining current observation networks[261], particularly in-situ moored buoys, with transition to include directional capabilities, and integration into an open-access global systems with consistent accuracy and quality control procedures across platforms[70,261]. Long records provide unique resources to study wave climate variability and trends, and more observations with comprehensive metadata records[70] can also have a positive impact on the homogeneity of derived wave data products (with the help of advanced calibration and homogenization techniques[262]). In addition, VOS records (which date back to the mid-nineteenth century) offer unique data that should be further used and validated—despite the subjective error and inhomogeneous sampling, VOS measurements are temporally consistent as operational practices have not changed[70].

Climate and wave model improvement

Regardless of the increase in observations, climate and wave models will continue to be vital tools for understanding the complex spatial-temporal features of historical and future wave climate. However, these models need to be improved in order to reduce the uncertainty of wave simulations associated with methodological factors. First, this improvement comes with reducing the uncertainty associated with surface wind projections, with one relevant aspect being the better representation of TC as this impacts estimations of low-probability extremes needed for infrastructures and coastal flooding management (as it has been seen for storm surge[263]). High-resolution (0.25° or less) global climate models[63] are needed to better capture TC properties. At high latitudes, it is also relevant to improve sea ice models to reduce existing biases and uncertainties in sea ice formation[264,265]. Second, we need to continue our efforts to improve the energy distribution across the wave spectrum[266], and better understand several key wave interaction processes with sea ice, currents, and winds at the ocean-atmospheric boundary layer[267], with one hot topic being the better characterization of wave/sea-ice interactions that are currently absent from Earth system models[210], meaning existing projections could be underestimating sea ice retreat and wave growth in partially sea ice covered areas. A more precise evaluation of the wave spectra is also needed to better characterize maximum wave heights, which is needed to assess possible impacts on freak waves[268], which are hazardous waves that are unusually larger than the surrounding waves. Overall, there is need for fundamental research with a multidisciplinary approach[261] (for example, the improvement of wave-ice parameterizations should be carried simultaneously with an improvement of ice models[269]). Also, this research needs to go hand in hand with the acquisition of more observations in other to develop better model parameterizations, and improve data assimilations and validation.

Improved understanding of extreme sea states with larger ensembles and better assessment of the uncertainty

Research on historical and future wind-wave climate should account for a better sampling of the internal natural climate variability, and the tail of the distribution to improve the understanding of the inter-decadal variability and reduce the uncertainty associated with 100-year return period events. The impacts of wave climate change will be felt most acutely in response to any changes in the properties of the extreme wave conditions. Therefore, it is the properties of the extremes that are of most interest to offshore and coastal infrastructure planners and operators. Moreover, larger ensembles with low to medium emission scenarios are required to reduce the uncertainty associated with these extreme wave conditions and identify climate change footprints[54]. With the imminent increase in CMIP6-derived wave studies, it also becomes important to carry out a comprehensive assessment of possible differences relative to the previous CMIP phase. The challenge posed by the large computational cost associated with the need for increasingly large wave ensembles can be addressed with the complementary use of machine learning techniques, which have been successfully applied to a large variety of modelling problems, including recent applications of wind-wave prediction[270]. Also, machine learning can potentially be implemented in areas with complex wave interactions such as sea ice-wave interaction, which are not covered by traditional statistical approaches.

Better coverage and improved high-resolution regional projections

While large-scale and global studies can be used to identify potential hotspot areas, they can be misleading if used directly to quantify wave-driven coastal impacts, which typically require a spatial resolution at kilometer scales[70]. Despite the advances made in region-wide local wave downscalling[271–273], efforts are needed to improve global coverage of regional and coastal assessments (in particular for low-lying and vulnerable populated coastlines), which need to make use of high-resolution downscaled wave projections that were driven from high-resolution forcing variables. Increased forcing resolution is particularly relevant in sheltered coastlines, where local weather patterns can dominate over the climate change signal[143]. However, increased resolution is not enough. The aforementioned need for fundamental wave modelling research becomes more pressing as getting closer to the coasts, where the more complex wave dynamics require the use of coupled wave-circulation models. It is critical to use enhanced coastal bathymetry information that accounts for local features[261,274], and to improve wave models to better capture relevant shallow processes such as wave breaking, and its interactions with coastal currents, sediment transport, and coastal erosion[275]. For example, the morphological adjustment to changes in offshore wave conditions can have an important impact on the resulting waves nearshore[5]. With the increase of regional wave projections, it would be ideal to integrate this information into an open-data system, such as the worlwide C3S CORDEX Grand Ensemble[276], to enable a much needed comprehensive quantitative assessment of regional-scale projections, the contribution of their uncertainty factors, and how it compares to global-scale results.

Integrating other marine and atmospheric drivers

Understanding change in waves is just one of many factors to resolve, as we seek to understand climate change impacts on our coasts and marine systems. From long-term sea level rise scenarios to wind-waves, coastal climate drivers across multiple temporal scales need to be considered as well as their interconnections. For example, over half of the coastlines exhibit dependencies between storm surge and wave extremes[277] which, together with intense precipitation or snowmelt, are key drivers of compound flooding[278]. There is a need to develop impact-based approaches that integrate (nonlinear) interactions and dependencies between waves and other marine/atmospheric drivers of the so-called compound events[279,280]. In addition, much of the attention of historical and future projected changes in wave characteristics has focused on the influence of climate driven changes in forcing atmospheric conditions. There is evidence to suggest that at the coast, these atmospheric forced driven changes will be overwhelmed by the influence that future changes in nearshore and coastal morphology, associated with SLR, reef growth rates and other coastal processes, have on wave characteristics[205,281]. For example, degraded coral reefs (that might result from weakened structure integrity due to acidification) can be more vulnerable to wave driven destruction and no long offer coastal protection from waves, leading to larger waves nearshore that drive greater coastal impacts[281,282]. Resolving these influences at global scale requires a step up in our observational and systems modelling capabilities.

References

1. Weisse, R. & von Storch, H. *Marine climate and climate change. Storms, winds, waves and storm surges* (Praxis Publishing, Chicheste, United Kingdom, 2010).
2. Holthuijsen, L. *Waves in oceanic and coastal waters* (Cambridge University Press, Cambridge, United Kingdom, 2007).
3. Thomson, J. & Rogers, W. E. Swell and sea in the emerging Arctic Ocean. *Geophys. Res. Lett.* **41**, 3136–3140, DOI: 10.1002/2014GL059983 (2014).
4. Ponce de León, S. & Guedes Soares, C. Extreme waves in the agulhas current region inferred from sar wave spectra and the swan model. *J. Mar. Sci. Eng.* **153**, DOI: 10.3390/jmse9020153 (2021).
5. Malito, J., Eidam, E. & Nienhuis, J. Increasing wave energy moves arctic continental shelves toward a new future. *J. Geophys. Res. Ocean.* **127**, e2021JC018374, DOI: 10.1029/2021JC018374 (2022).
6. Dodet, G. *et al.* The contribution of wind-generated waves to coastal sea-level changes. *Surv. Geophys.* **40**, 1563–1601, DOI: 10.1007/s10712-019-09557-5 (2019).
7. Stive, M. J. *et al.* Variability of shore and shoreline evolution. *Coast. Eng.* **47**, 211–235, DOI: 10.1016/S0378-3839(02)00126-6 (2002).
8. Grifoll, M., Martínez de Osés, F. & Castells, M. Potential economic benefits of using a weather ship routing system at short sea shipping. *WMU J. Marit. Aff.* **17**, 195–211, DOI: 10.1007/s13437-018-0143-6 (2018).
9. Kamranzad, B., Amarouche, K. & Akpinar, A. Linking the long-term variability in global wave energy to swell climate and redefining suitable coasts for energy exploitation. *Nat. Sci. Reports* **12**, 14692, DOI: 10.1038/s41598-022-18935-w (2022).
10. Galluta, D., Tahmasbi Fard, M., Gutierrez Soto, M. & He, J. Recent advances in wave energy conversion systems: from wave theory to devices and control strategies. *Ocean. Eng.* **252**, 111105, DOI: 10.1016/j.oceaneng.2022.111105 (2022).
11. Spyros, F. Wave energy converters in low energy seas: current state and opportunities. *Renew. Sustain. Energy Rev.* **162**, 112448, DOI: 10.1016/j.rser.2022.112448 (2022).
12. Cisneros-Montemayor, A. M. & et al. Enabling conditions for an equitable and sustainable blue economy. *Nature* **591**, 396–401, DOI: 10.1038/s41586-021-03327-3 (2021).
13. Wenhai, L. & et al. Successful Blue Economy Examples With an Emphasis on International Perspectives. *e* 662–671, DOI: 10.3389/fmars.2019.00261 (2019).
14. Hemer, M. A., Church, J. A. & Hunter, J. R. Variability and trends in the directional wave climate of the Southern Hemisphere. *Int. J. Climatol.* **30**, 475–491, DOI: 10.1002/JOC.1900 (2010).
15. Almar, R. & et al. Influence of el niño on the variability of global shoreline position. *Nat. Commun.* **14**, DOI: 10.1038/s41467-023-38742-9 (2023).
16. Barnard, P. L. *et al.* Extreme oceanographic forcing and coastal response due to the 2015–2016 El Niño. *Nat. Commun. 2017 8:1* **8**, 1–8, DOI: 10.1038/ncomms14365 (2017).
17. Harley, M. D. & et al. Extreme coastal erosion enhanced by anomalous extratropical storm wave direction. *Nat. Sci. Reports* **7**, 6033, DOI: 10.1038/s41598-017-05792-1 (2017).
18. Vitousek, S. *et al.* Doubling of coastal flooding frequency within decades due to sea-level rise. *J. Geophys. Res. Earth Surf.* **126**, e2019JF005506, DOI: 10.1029/2019JF005506 (2021).
19. Almar, R. *et al.* A global analysis of extreme coastal water levels with implications for potential coastal overtopping. *Nat. Commun.* **12**, 3775, DOI: 10.1038/s41467-021-24008-9 (2021).
20. Vitousek, S., Barnard, C. H., Fletcher, Frazer, N., Erikson, L. & Storlazzi. Doubling of coastal flooding frequency within decades due to sea-level rise. *Nat. Sci. Reports* **7**, 1399, DOI: 10.1038/s41598-017-01362-7 (2017).
21. Bugnot, A. & et al. Current and projected global extent of marine built structures. *Nat. Sustain.* **4**, 33–41, DOI: 10.1038/s41893-020-00595-1 (2019).
22. Sierra, J. & Casas-Prat, M. Analysis of potential impacts on coastal areas due to changes in wave conditions. *Surv. Geophys.* **124**, 861–879, DOI: 10.1007/s10584-014-1120-5 (2014).
23. Heij, C. & Knapp, S. Effects of wind strength and wave height on ship incident risk: Regional trends and seasonality. *Transp. Res. Part D: Transp. Environ.* **37**, 29–39, DOI: 10.1016/j.trd.2015.04.016 (2015).

24. Chust, G. e. Climate regime shifts and biodiversity redistribution in the bay of biscay. *Sci. Total. Environ.* **803**, 149622, DOI: 10.1016/j.scitotenv.2021.149622 (2022).

25. Cavaleri, L., Fox-Kemper, B. & Hemer, M. Wind waves in the coupled climate system. *Bull. Am. Meteorol. Soc.* **93**, 1651–1661, DOI: 10.1175/BAMS-D-11-00170.1 (2012).

26. Zou, Z. *et al.* Effects of swell waves on atmospheric boundary layer turbulence: a low wind field study. *J. Geophys. Res. Ocean.* **124**, 5671–5685 (2019).

27. IPCC. *Climate Change 2013: The Physical Science Basis. Contribution of Working Group I to the Fifth Assessment Report of the Intergovernmental Panel on Climate Change [Stocker, T.F., D. Qin, G.-K. Plattner, M. Tignor, S.K. Allen, J. Boschung, A. Nauels, Y. Xia, V. Bex and P.M. Midgley (eds.)]* (Cambridge University Press, Cambridge, United Kingdom and New York, NY, USA, 1535 pp., 2013).

28. Hemer, M., Wang, X., Weisse, R. & Swail, V. Advancing wind-waves climate science: the cowclip project. *Bull. Am. Meteorol. Soc.* **93**, 791–796, DOI: 10.1175/BAMS-D-11-00184.1 (2012).

29. Dodet, G., Piolle, J.-F., Quilfen, Y. & et al. The sea state cci dataset v1: towards a sea state climate data record based on satellite observations. *Earth Syst. Sci. Data* **12**, 1929–1951, DOI: 10.5194/essd-12-1929-202 (2020).

30. Le Traon, Y. & et al. From observation to information and users: The copernicus marine service perspective. *Syst. Rev. Article* **6**, DOI: 10.3389/fmars.2019.00234 (2019).

31. Morim, J. *et al.* A global ensemble of ocean wave climate statistics from contemporary wave reanalysis and hindcasts. *Nat. Sci. Data* **9**, 358 (2022).

32. Young, I. & Ribal, A. Multiplatform evaluation of global trends in wind speed and wave height. *Science* **80**, 548–552 (2019).

33. Hemer, M., Fan, Y., Mori, N., Semedo, A. & Wang, X. Projected changes in wave climate from a multi-model ensemble. *Nat. Clim. Chang.* **3**, 471–476 (2013).

34. Morim, J., Hemer, M., Cartwright, N., Strauss, D. & Andutta, F. On the concordance of 21st century wind-wave climate projections. *Glob. Planet. Chang.* **167**, 160–171, DOI: 10.1016/J.GLOPLACHA.2018.05.005 (2018).

35. Morim, J. *et al.* Robustness and uncertainties in global multivariate wind-wave climate projections. *Nat. Clim. Chang.* **9**, 711–718, DOI: 10.1038/s41558-019-0542-5 (2019).

36. Morim, J. *et al.* A global ensemble of ocean wave climate projections from cmip5-driven models. *Nat. Sci. Data* **7** (2020).

37. Morim, J. *et al.* Global-scale changes to extreme ocean wave events due to anthropogenic warming. *Environ. Res. Lett.* **16**, 074056, DOI: 10.1088/1748-9326/AC1013 (2021).

38. Odériz, I. *et al.* Transitional wave climate regions on continental and polar coasts in a warming world. *Nat. Clim. Chang.* **12**, 662–671, DOI: 10.1038/s41558-022-01389-3 (2022).

39. IPCC. *Climate Change 2021: The Physical Science Basis. Contribution of Working Group I to the Sixth Assessment Report of the Intergovernmental Panel on Climate Change [Masson-Delmotte, V., P. Zhai, A. Pirani, S.L. Connors, C. Péan, S. Berger, N. Caud, Y. Chen, L. Goldfarb, M.I. Gomis, M. Huang, K. Leitzell, E. Lonnoy, J.B.R. Matthews, T.K. Maycock, T. Waterfield, O. Yelekçi, R. Yu, and B. Zhou (eds.)]* (Cambridge University Press, Cambridge, United Kingdom and New York, NY, USA, 1535 pp., 2021).

40. Walden, H., Hogben, N., Burkhart, D. R., M.D. & Warnsink, Y. Y., W.H. Long term variability. *Fourth Int. Ship Struct. Congr. 49-59 (Royal Inst. Nav. Archit.* (1970).

41. Gulev, S. & Grigorieva, V. Last century changes in ocean wind wave height from global visual wave data. *Geophys. Res. Lett.* **31**, 1–4 (2004).

42. Ardhuin, A., Chapron, B. & Collard, F. Observation of swell dissipation across oceans. *Geophys. Res. Lett.* **36**, DOI: 10.1029/2008GL037030 (2009).

43. Hauser, D. & et al. New observations from the swim radar on-board cfosat: Instrument validation and ocean wave measurement assessment. *IEEE Transactions on Geosci. Remote. Sens.* **59**, 5–26, DOI: 10.1109/TGRS.2020.2994372 (2021).

44. Timmermans, B. W., Gommenginger, C. P., Dodet, G. & Bidlot, J.-R. Global Wave Height Trends and Variability from New Multimission Satellite Altimeter Products, Reanalyses, and Wave Buoys. *Geophys. Res. Lett.* **47**, e2019GL086880, DOI: 10.1029/2019GL086880 (2020).

45. Gemmrich, J., Thomas, B. & Bouchard, R. Observational changes and trends in northeast Pacific wave records. *Geophys. Res. Lett.* **38**, 22601, DOI: 10.1029/2011GL049518 (2011).

46. Young, Y. & Ribal, A. Can multi-mission altimeter datasets accurately measure long-term trends in wave height? *Remote. Sens.* **14**, 974, DOI: 10.3390/rs14040974 (2022).

47. Jiang, H. Evaluation of altimeter undersampling in estimating global wind and wave climate using virtual observation. *Remote. sensing environment* **245**, 111840, DOI: 10.1016/j.rse.2020.111840 (2020).

48. Aviso+. Timeline of modern radar altimetry missions, version 2023/06. *Intergov. Panel for Clim. Chang.* , DOI: 10.24400/527896/A02-2022.001 (2022).

49. Collard, F., Ardhuin, F. & Chapron, B. Monitoring and analysis of ocean swell fields from space: New methods for routine observations. *J. Geophys. Res. Ocean.* **114**, DOI: 10.1029/2008JC005215 (2009).

50. Cao, C., Chen, G., Qian, C. & Shang, J. Spatiotemporal variability and climate teleconnections of global ocean wave power. *Front. Mar. Sci.* DOI: 10.3389/fmars.2022.900950 (2022).

51. Izaguirre, C., Méndez, F. J., Menéndez, M. & Losada, I. J. Global extreme wave height variability based on satellite data. *Geophys. Res. Lett.* **38**, DOI: 10.1029/2011GL047302 (2011).

52. Shimura, T., Mori, N. & Mase, H. Ocean Waves and Teleconnection Patterns in the Northern Hemisphere. *J. Clim.* **26**, 8654–8670, DOI: 10.1175/JCLI-D-12-00397.1 (2013).

53. Echevarria, E. R., Hemer, M. A., Holbrook, N. J. & Marshall, A. G. Influence of the Pacific-South American Modes on the Global Spectral Wind-Wave Climate. *J. Geophys. Res. Ocean.* **125**, e2020JC016354, DOI: 10.1029/2020JC016354 (2020).

54. Morim, J. *et al.* Understanding uncertainties in contemporary and future extreme wave events for broad-scale impact and adaptation planning. *Sci. Adv.* **9**, eade3170, DOI: 10.1126/sciadv.ade3170 (2023).

55. Erikson, M. J., L. *et al.* Global ocean wave fields show consistent regional trends between 1980 and 2014 in a multi-product ensemble. *Nat. Commun. Earth Environ.* **3**, DOI: 10.1038/s43247-022-00654-9 (2022).

56. Gavrikov, A. e. Ras-naad: 40-yr high-resolution north atlantic atmospheric hindcast for multipurpose applications (new dataset for the regional mesoscale studies in the atmosphere and the ocean). *J. Appl. Meteorol. Climatol.* **59**, 793–817, DOI: 10.1175/JAMC-D-19-0190.1 (2020).

57. Alday, M., Accensi, M., Arduhin, F. & Dodet, G. A global wave parameter database for geophysical applications. part 3: Improved forcing and spectral resolution. *Ocean. Model.* **166**, 101848, DOI: 10.1016/j.ocemod.2021.101848 (2021).

58. Ardhuin, F. *et al.* Comparison of wind and wave measurements and mnodels in the western mediterranean sea. *Ocean. Eng.* **34**, 526–541, DOI: 10.1016/j.oceaneng.2006.02.008 (2007).

59. Hodges, K., Cobb, A. & Vidale, P. How well are tropical cyclones represented in reanalysis datasets? *J. Clim.* **30**, 5243–5264, DOI: 10.1175/JCLI-D-16-0557.1 (2017).

60. Slocum, C., Naufal Razin, M., Knaff, J. & Stow, J. Does era5 mark a new era for resolving the tropical cyclone environment? *J. Clim.* **35**, 3547–3564, DOI: 10.1175/JCLI-D-22-0127.1 (2022).

61. Dulac, W., Cattiaux, J., Chauvin, F., Bourdin, S. & Fromang, S. How realistic are tropical cyclones in the era5 reanalysis? *EGU22-5755, updated on 04 May 2023* 1025–1039, DOI: 10.5194/egusphere-egu22-5755 (2023).

62. Han, Z. *et al.* Evaluation on the applicability of era5 reanalysis dataset to tropical cyclones affecting shanghai. *Quaterly J. Royal Meteorol. Soc.* **16**, 1025–1039, DOI: 10.1007/s11707-022-0972-7 (2022).

63. Timmermans, B., Stone, D., Wehner, M. & Krishnan, H. Impact of tropical cyclones on modeled extreme wind-wave climate. *Geophys. Res. Lett.* **44**, 1393–1401, DOI: 10.1002/2016GL071681 (2017).

64. Law-Chune, S. *et al.* Waverys: a cmems global wave reanalysis during the altimetry period. *Ocean. Dyn.* **71**, 357–378, DOI: 10.1007/s10236-020-01433-w (2021).

65. Aarnes, O., Abdalla, S., Jean-Raymond, B. & Breivik, O. Marine wind and wave height trends at different era-interim forecast ranges. *J. climate* **28**, 819–837, DOI: 10.1175/JCLI-D-14-00470.1 (2015).

66. Casas-Prat, M. *et al.* Effects of internal climate variability on historical ocean wave height trend assessment. *Front. Mar. Sci.* **9**, DOI: 10.3389/fmars.2022.847017 (2022).

67. Meucci, A., Young, I. R., Aarnes, O. J. & Breivik, Ø. Comparison of Wind Speed and Wave Height Trends from Twentieth-Century Models and Satellite Altimeters. *J. Clim.* **33**, 611–624, DOI: 10.1175/JCLI-D-19-0540.1 (2020).

68. Sharmar, V. & Markina, M. Evaluation of interdecadal trends in sea ice, surface winds and ocean waves in the Arctic in 1980-2019. *RUSSIAN JOURNAL OF EARTH SCIENCES* **21**, 2021, DOI: 10.2205/2020ES000741 (2021).

69. Stopa, J., Ardhuin, F., Stutzmann, E. & Lecocq, T. Sea state trends and variability: consistency between models, altimetres, buoys, and seismic data (1979-2016). *J. Geophys. Res. Ocean.* **124**, 3923–3940 (2019).

70. Ardhuin, F. *et al.* Observing sea states. *Front. Mar. Sci.* DOI: 10.3389/fmars.2019.00124 (2019).

71. Herbach, H., Bell, B., Berrisford, P. & *et al*. The era5 global reanalysis. *Quaterly J. Royal Meteorol. Soc.* **146**, 1999–2049, DOI: 10.1001/qj.3803 (2020).

72. Hersbach, H. & et al. Operational global reanalysis: progress, future directions and synergies with NWP. *ECMWF ERA Rep. Ser.* **27** (1986).

73. Saha, S. *et al.* The ncep climate forecast system version 2. *J. Clim.* **146**, 2185–2208, DOI: 10.1175/JCLI-D-12-00823.1 (2014).

74. Chawla, A., Spindler, D. & Tolman, H. Validation of a thirty year wave hindcast using the climate forecast system reanalysis winds. *Ocean. Model.* **70**, 189–206, DOI: 10.1016/j.ocemod.2012.07.005 (2010).

75. Casas-Prat, M. *et al.* A 100-member ensemble simulations of global historical (1951-2010) wave heights. *Nat. Sci. Data* **10**, DOI: 10.1038/s41597-023-02058-6 (2023).

76. Patra, A., Dodet, G. & Accensi, M. Historical global ocean wave data simulated with cmip6 anthropogenic and natural forcings. *Nat. Sci. Data* **10**, 325, DOI: 10.12770/0983962b-4acc-4f8f-9484-e2195029b87b (2023).

77. Eyring, V. & et al. Overview of the Coupled Model Intercomparison Project Phase 6 (CMIP6) experimental design and organization. *Geosci. Model. Dev.* **9**, 2016, DOI: 10.5194/gmd-9-1937-2016 (2016).

78. van Vuuren, D. & et al. A new scenario framework for climate change research: scenario matrix architecture. *Clim. Chang.* **122**, 373–386, DOI: 10.1007/s10584-013-0906-1 (2014).

79. Song, Z. *et al.* Centuries of monthly and 3-hourly global ocean wave data for past, present, and future climate research. *Nat. Sci. Data* **7**, 1 (2020).

80. Mori, J., Hemer, M., Andutta, F., Shimura, T. & Cartwright, N. Skill and uncertainty in surface wind fields from general circulation models: Intercomparison of bias between agcm, aogcm and esm global simulations. *Int. J. Climatol.* **40**, 2659–2673, DOI: 10.1002/joc.6357 (2019).

81. Lobeto, H., Menendez, M. & Losada, I. J. Projections of Directional Spectra Help to Unravel the Future Behavior of Wind Waves. *Front. Mar. Sci.* DOI: 10.3389/fmars.2021.655490 (2021).

82. Lobeto, H., Menendez, M. & Losada, I. J. The effect of climate change on wind-wave directional spectra. *Glob. Planet. Chang.* **213**, 103820, DOI: 10.1038/s41598-021-86524-4 (2022).

83. Erikson, L. H. and et al. Ocean wave time-series data simulated with a global-scale numerical wave model under the influence of projected cmip6 wind and sea ice fields. *U.S. Geol. Surv. data* DOI: 10.5066/P9KR0RFM. (2022).

84. Kumar, R., Lemos, G., Semedo, A. & Alsaaq, F. Parameterization-driven uncertainties in single-forcing, single-model wave climate projections from a cmip6-derived dynamic ensemble. *Climate* **10**, DOI: 10.3390/cli10040051 (2022).

85. Meucci, A., Young, I., Hemer, M., Trenham, C. & Watterson, I. 140 years of global ocean wind-wave climate derived from cmip6 access-cm2 and ec-earth3 gcms: Global trends, regional changes, and future projections. *J. Clim.* 1605–1631, DOI: 10.1175/JCLI-D-21-0929.1 (2023).

86. Taylor, K. & et al. A overview of cmip5 and the experiment design. *Bull. Am Meteorol Soc* **122**, 485–498, DOI: 10.1007/s10584-013-0906-1 (2012).

87. Roberts, M. & et al. Projected future changes in tropical cyclones usingthe cmip6 highresmip multimodel ensemble. *Geophys. Res. Lett.* **47**, e2020GL088662, DOI: 10.1029/2020GL088662 (2020).

88. Taylor, K., Stouffer, G. & Meehl, G. An overview of cmip5 and the experiment design. *Bull. Am. Meteorol. Soc.* **93**, 485–498, DOI: 10.1175/BAMS-D-11-00094.1 (2012).

89. Shimura, T., Mori, N. & Mase, H. Future Projections of Extreme Ocean Wave Climates and the Relation to Tropical Cyclones: Ensemble Experiments of MRI-AGCM3.2H. *J. Clim.* **28**, 9838–9856, DOI: 10.1175/JCLI-D-14-00711.1 (2015).

90. Shimura, T., Pringle, W., Mori, N., MIyashita, T. & Yoshida, K. Seamless projections of global storm surge and ocean waves under a warming climate. *Geophys. Res. Lett.* **49**, e2021GL097427, DOI: 10.1029/2021GL097427 (2015).

91. Haarsma, R. & et al. High resolution model intercomparison project (highresmip v1.0) for cmip6. *Geosci. Model. Dev.* **9**, 4185–4208, DOI: 10.5194/gmd-9-4185-2016 (216).

92. Parker, K. and Erikson, L. and Thomas, J. and Nederhoff, K. and Barnard, P. and Muis, S. Relative contributions of water-level components to extreme water levels along the us southeast atlantic coast from a regional-scale water-level hindcast. *Nat. Hazards* **874**, DOI: 10.1007/s11069-023-05939-6 (2023).

93. IPCC. Special Report on the Ocean and Cryosphere in a Changing Climate —. Tech. Rep., Intergovernmental Panel for Climate Change (2019).

94. Casas-Prat, M., Wang, X. L. & Swart, N. CMIP5-based global wave climate projections including the entire Arctic Ocean. *Ocean. Model.* **123**, 66–85, DOI: 10.1016/j.ocemod.2017.12.003 (2018).

95. Casas-Prat, M. & Wang, X. L. Projections of Extreme Ocean Waves in the Arctic and Potential Implications for Coastal Inundation and Erosion. *J. Geophys. Res. Ocean.* **125**, e2019JC015745, DOI: 10.1029/2019JC015745 (2020).

96. Casas-Prat, M. & Wang, X. Sea ice retreat contributes to projected increases in extreme arctic ocean surface waves. *Geophys. Res. Lett.* **45**, DOI: 10.1029/2020GL088100 (2020).

97. Jiang, X., Xie, B., Bao, Y. & Song, Z. Global 3-hourly wind-wave and swell data for wave climate and wave energy resource research from 1950 to 2100. *Nat. Sci. Data* **10**, 1 (2023).

98. Christensen, J. H. & Christensen, O. B. A summary of the prudence model projections of changes in european climate by the end of this century. *Clim. Chang.* **81**, 7–30, DOI: 10.1007/s10584-006-9210-7 (2007).

99. van der Linden, P. & (eds.), J. M. Ensembles: climate change and its impacts: summary of research and results from the ensembles project. *Met Off. Hadley Centre, FitzRoy Road, Exeter EX1 3PB, UK* 160pp (2009).

100. Outen, S. & Sobolowski, S. Extreme wind projections over europe from the euro-cordex regional climate models. *Weather. climate extremes* **33**, 100363, DOI: 10.1016/j.wace.2021.100363 (2021).

101. Kulp, S. & Strauss, B. New elevation data triple estimates of global vulnerability to sea-level rise and coastal flooding. *Nat. Commun.* **10**, 4844, DOI: 10.1038/s41467-019-12808-z (2019).

102. Badriana, M. & Lee, H. S. Multimodel ensemble projections of wave climate in the western north pacific using cmip6 marine surface winds. *J. Mar. Sci. Eng.* **9**, 835, DOI: 10.3390/jmse9080835 (2021).

103. Liu, J., Meucci, A. & Young, I. Projected wave climate of bass strait and south-east australia by the end of the twenty-first century. *Clim. Dyn.* **60**, 393–407, DOI: 10.1007/s00382-022-06310-4 (2023).

104. Pourali, M., Kavianpour, M., Kamranzad, B. & Alizadeh, M. Future variabiilty of wave energy in the gulf of oman using a high resolution cmip6 climate model. *Energy* **262**, 125552, DOI: 10.1016/j.energy.2022.125552 (2023).

105. UNFCCC. Report of the structured expert dialogue on the 2013-2015 review framework convention on climate change. Tech. Rep. (2015).

106. Patra, A., Min, S., Kumar, P. & Wang, X. Changes in extreme ocean wave heights under 1.5c, 2c, and 3c global warming. *Weather. Clim. Extrem.* **33**, 100358, DOI: 10.1016/j.wace.2021.100358 (2021).

107. Shepherd, T. & et al. Storylines: an alternative approach to representing uncertainty in physical aspects of climate change. *Clim. Chang.* **151**, 555–571, DOI: 10.1007/s10584-018-2317-9 (2018).

108. Sillman, J. & et al. Physical modeling supporting a storyline approach. *CICERO Work. Rep.* 29 pp. (2019).

109. Neu, H. J. Interannual variations and longer-term changes in the sea state of the North Atlantic from 1970 to 1982. *J. Geophys. Res. Ocean.* **89**, 6397–6402, DOI: 10.1029/JC089IC04P06397 (1984).

110. Allan, J. & Komar, P. Are ocean wave heights increasing in the eastern North Pacific? *Eos, Transactions Am. Geophys. Union* **81**, 561–567, DOI: 10.1029/EO081I047P00561-01 (2000).

111. Gulev, S. & Hasse, L. Changes of wind waves in the north atlantic over the last 30 years. *Int. J. Climatol.* **19**, 1091–1117 (1999).

112. Wang, X. L., Feng, Y. & Swail, V. R. North Atlantic wave height trends as reconstructed from the 20th century reanalysis. *Geophys. Res. Lett.* **39**, DOI: 10.1029/2012GL053381 (2012).

113. Woolf, D. Variability and predictability of the north atlantic wave climate. *J. Geophys. Res.* **107**, 3145 (2002).

114. Hanafin, J. *et al.* Phenomenal sea states and swell from a north atlantic storm in february 2011: A comprehensive analysis. *Bull. Am. Meteorol. Soc.* **93**, DOI: 10.1175/BAMS-D-11-00128.1 (2012).

115. Almar, R. *et al.* Response of the Bight of Benin (Gulf of Guinea, West Africa) coastline to anthropogenic and natural forcing, Part1: Wave climate variability and impacts on the longshore sediment transport. *Cont. Shelf Res.* **110**, 48–59, DOI: 10.1016/J.CSR.2015.09.020 (2015).

116. Cavaleri, L. & Sclavo, M. The calibration of wind and wave model data in the mediterranean sea. *Coast. Eng.* **53**, 613–627, DOI: 10.1016/j.coastaleng.2005.12.006 (2006).

117. Mentaschi, L., Besio, G., Cassola, F. & Mazzino, A. Performance evaluation of wavewatch iii in the mediterreanean sea. *Ocean. Model.* **90**, 82–94, DOI: 10.1016/j.ocemod.2015.04.003 (2015).

118. Izaguirre, C., Mendez, F., Menendez, M., Luceño, A. & Losada, I. Extreme wave climate variability in southern europe using satellite data. *J. Geophys. Res.* **115**, C04009 (2010).

119. Barbariol, F. & et al. Wind waves in the mediterranean sea: and era5 reanalysis wind-based climatology. *Front. Mar. Sci.* DOI: 10.3389/fmars.2021.760614 (2021).

120. Pérez-Gómez, B. & et al. Understanding sea level processes during western mediterranean storm gloria. *Front. Mar. Sci.* **8** (2021).

121. Bacon, S. & Carter, D. J. Wave climate changes in the North Atlantic and North Sea. *Int. J. Climatol.* **11**, 545–558, DOI: 10.1002/JOC.3370110507 (1991).

122. Bouws, E., Jannink, D. & Komen, G. The increasing wave height in the North Atlantic Ocean. *Bull. Am. Soc.* **77**, 2275–2278, DOI: 10.1175/1520-0477(1996)077<2275:TIWHIT>2.0.CO;2 (1996).

123. Carter, D. & Draper, L. Has the north-east Atlantic become rougher? *Nature* **332**, 494 (1988).

124. Gunther, H. *et al.* The wave climate of the Northeast Atlantic over the period 1955-1994: The WASA wave hindcast. *The Glob. Atmosphere Ocean. Syst.* **77** (1997).

125. Wang, X. L. & Swail, V. R. Trends of Atlantic Wave Extremes as Simulated in a 40-Yr Wave Hindcast Using Kinematically Reanalyzed Wind Fields in: Journal of Climate Volume 15 Issue 9 (2002). *J. Clim.* **15**, 1020–1035 (2002).

126. Bertin, X., Prouteau, E. & Letetrel, C. A significant increase in wave height in the north atlantic ocean over the 20th century. *Glob. Planet. Chang.* **106**, 77–83 (2013).

127. Sharmar, V. D., Markina, M. Y. & Gulev, S. K. Global Ocean Wind-Wave Model Hindcasts Forced by Different Reanalyzes: A Comparative Assessment. *J. Geophys. Res. Ocean.* **126**, e2020JC016710, DOI: 10.1029/2020JC016710 (2021).

128. Hochet, A., Dodet, G., Sévellec, F., Bouin, M.-N. & Patra, A., A. amd Ardhuin. Time of emergence for altimetry-based significant wave height changes in the north atlantic. *Geophys. Res. Lett.* **50**, e2022GL102348., DOI: 10.1029/2022GL102348 (2023).

129. Lionello, P. & Sanna, A. Mediterranean wave climate variability and its links with nao and indian monsoon. *Clim. Dyn.* **25**, 611–623 (2005).

130. Bromirski, P. D. & Cayan, D. R. Wave power variability and trends across the North Atlantic influenced by decadal climate patterns. *J. Geophys. Res. Ocean.* **120**, 3419–3443, DOI: 10.1002/2014JC010440 (2015).

131. Freitas, A., Bernardino, M. & Guedes Soares, C. The influence of the arctic oscillation on north atlantic wind and wave climate by the end of the 21st century. *Ocean. Eng.* **246**, 110634 (2022).

132. Hochet, A., Dodet, G., Ardhuin, F., Hemer, M. & Young, I. Sea state decadal variability in the north atlantic: A review. *Climate* **9**, 173, DOI: 10.3390/cli9120173 (2021).

133. Castelle, B., Dodet, G., Masselink, G. & Scott, T. A new climate index controlling winter wave activity along the Atlantic coast of Europe: The West Europe Pressure Anomaly. *Geophys. Res. Lett.* **44**, 1384–1392, DOI: 10.1002/2016GL072379 (2017).

134. Izaguirre, C., Mendez, F., Menendez, M., & Losada, I. Global extreme wave height variability based on satellite data. *Geophys. Res. Lett.* **38** (2011).

135. Reguero, B. G., Losada, I. J. & Méndez, F. J. A recent increase in global wave power as a consequence of oceanic warming. *Nat. Commun. 2019 10:1* **10**, 1–14, DOI: 10.1038/s41467-018-08066-0 (2019).

136. Silva, A. *et al.* Climate-induced variability in south atlantic wave direction over the past three millennia. *Nat. Sci. Reports* **10**, 18553, DOI: 10.1038/s41598-020-75265-5 (2020).

137. Morales-Márquez, V., Orfila, A., Simarro, G. & Marcos, M. Extreme waves and climatic patterns of variability in the eastern North Atlantic and Mediterranean basins. *Ocean. Sci.* **16**, 1385–1398, DOI: 10.5194/OS-16-1385-2020 (2020).

138. Lemos, G., Menendez, M., Semedo, A., Miranda, P. M. & Hemer, M. On the decreases in North Atlantic significant wave heights from climate projections. *Clim. Dyn.* **57**, 2301–2324, DOI: 10.1007/S00382-021-05807-8/TABLES/7 (2021).

139. Perez, J., Menendez, M., Camus, P., Mendez, F. & Losada, I. Statistical multi-model climate projections of surface ocean waves in europe. *Ocean. Model.* **96**, 161–170, DOI: 10.1016/j.ocemod.2015.06.001 (2015).

140. Meucci, A., Young, I., Hemer, M., Kirezci, E. & Ranasinghe, R. Projected 21st century changes in extreme wind-wave events. *Sci. Adv.* **6**, DOI: 10.1126/sciadv.aaz7295 (2020).

141. Lemos, G. *et al.* Mid-twenty-first century global wave climate projections: results from a dynamic cmip5 based ensemble. *Glob. Planet. Chang.* **172**, 69–87, DOI: 10.1016/j.gloplacha.2018.09.011 (2019).

142. Metaschi, L., Vousdoukas, M., Voukouvalas, E., Dosio, A. & Feyen, L. Global changes of extreme coastal wave energy fluxes triggered by intensified teleconnection patterns. *Geophys. Res. Lett.* **44**, 2416–2426, DOI: 10.1002/2016GL072488 (2017).

143. Bricheno, L. & Wolf, J. Future wave conditions of europe, in response to high-end climate change scenarios. *J. Geophys. Res. Ocean.* **123**, 8762–8791, DOI: 10.1029/2018JC013866 (2018).

144. De Leo, F., Besio, G. & Mentaschi, L. Trends and variability of ocean waves under RCP8.5 emission scenario in the Mediterranean Sea. *Ocean. Dyn.* **71**, 97–117, DOI: 10.1007/S10236-020-01419-8/TABLES/4 (2021).

145. Lira-Loarca, A., Ferrai, F., Mazzino, A. & Besio, G. Future wind and wave energy resources and exploitability in the mediterranean sea by 2100. *Appl. Energy* **302**, 117492, DOI: 10.1016/j.apenergy.2021.117492 (2021).

146. Lira-Loarca, A. & Besio, G. Future changes and seasonal variability of the directional wave spectra in the mediterranean sea for the 21st century. *Environ. Res. Lett.* **17**, 104015, DOI: 10.1088/1748-9326/ac8ec4 (2022).

147. Casas-Prat, M. & Sierra, J. P. Projected future wave climate in the NW Mediterranean Sea. *J. Geophys. Res. Ocean.* **118**, 3548–3568, DOI: 10.1002/JGRC.20233 (2013).

148. Toomey, T., Amores, A., Marta, M., Orfila, A. & Romero, R. Coastal hazards of tropical-like cyclones over the mediterranean sea. *J. Geophys. Res. Ocean.* **12**, DOI: 10.1029/2021JC017964 (2022).

149. Reguero, B. G., Losada, I. J. & Méndez, F. J. A global wave power resource and its seasonal, interannual and long-term variability. *Appl. Energy* **148**, 366–380, DOI: 10.1016/J.APENERGY.2015.03.114 (2015).

150. Young, I. Seasonal variability of the global ocean wind and wave climate. *Int. J. Climatol.* **19**, 931–950 (1999).

151. Gulev, S. Assessment of the reliability of wave observations from voluntary observing ships: Insights from teh validation of a global wind wave climatology based on voluntary observing ship data. *J. Geophys. Res.* **108**, 3236 (2003).

152. Menéndez, M., Méndez, F. J., Losada, I. J. & Graham, N. E. Variability of extreme wave heights in the northeast Pacific Ocean based on buoy measurements. *Geophys. Res. Lett.* **35**, DOI: 10.1029/2008GL035394 (2008).

153. Ruggiero, P., Komar, P. D. & Allan, J. C. Increasing wave heights and extreme value projections: The wave climate of the U.S. Pacific Northwest. *Coast. Eng.* **57**, 539–552, DOI: 10.1016/J.COASTALENG.2009.12.005 (2010).

154. Echevarria, E. R., Hemer, M. A. & Holbrook, N. J. Seasonal Variability of the Global Spectral Wind Wave Climate. *J. Geophys. Res. Ocean.* **124**, 2924–2939, DOI: 10.1029/2018JC014620 (2019).

155. Sasaki, W. Changes in wave energy resources around japan. *Geophys. Res. Lett.* **39**, 1, DOI: 10.1029/2012GL053845 (2012).

156. Woo, H.-J. & Park, K.-A. Long-term trend of satellite-observed significant wave height and impact on ecosystem in the east/japan sea. *Nat. Sci. Reports* **143**, 1–14, DOI: 10.1016/j.dsr2.2016.09.003 (2017).

157. Wu, L., Wang, X. L. & Feng, Y. Historical wave height trends in the South and East China Seas, 1911–2010. *J. Geophys. Res. Ocean.* **119**, 4399–4409, DOI: 10.1002/2014JC010087 (2014).

158. Young, I. R., Fontaine, E., Liu, Q. & Babanin, A. V. The Wave Climate of the Southern Ocean. *J. Phys. Oceanogr.* **50**, 1417–1433, DOI: 10.1175/JPO-D-20-0031.1 (2020).

159. Shand, T. D. *et al.* Long Term Trends in NSW Coastal Wave Climate and Derivation of Extreme Design Storms. In *2011 NSW Coastal Conference* (2011).

160. Stopa, J. E. & Cheung, K. F. Periodicity and patterns of ocean wind and wave climate. *J. Geophys. Res. Ocean.* **119**, 5563–5584, DOI: 10.1002/2013JC009729 (2014).

161. Kaur, S., Kumar, P., Weller, E., Min, S. & Jin, J. Multi-model ensemble projections of extreme ocean wave heights over the indian ocean. *Clim. Dyn.* **56**, 2163–2180 (2021).

162. Barnard, P. L. *et al.* Coastal vulnerability across the Pacific dominated by El Niño/Southern Oscillation. *Nat. Geosci. 2015 8:10* **8**, 801–807, DOI: 10.1038/ngeo2539 (2015).

163. Shimura, T., Mori, N. & Hemer, M. Variability and future decreases in winter wave heights in the western north pacific. *Geophys. Res. Lett.* (2016).

164. Li, D. *et al.* Dynamical projections of the mean and extreme wave climate in the bohai sea, yellow sea and east china sea. *Front. Mar. Sci.* DOI: 10.3389/fmars.2022.844113 (2022).

165. Dowdy, A., Mills, G., Timbal, B. & Wang, Y. Fewer large waves projected for eastern australia due to decreasing storminess. *Nat. climate change* **4**, 282–286, DOI: 10.1038/nclimate2142 (2014).

166. Lobeto, H., Menendez, M. & Losada, I. J. Future behavior of wind wave extremes due to climate change. *Sci. Reports* **11**, DOI: 10.1038/s41598-021-86524-4 (2021).

167. Taniguchi, K. & Tajima, Y. Variations in extreme wave events near a south pacific island under global warming: case study of tropical cyclone tomas. *Prog Earth Planet Sci* **7**, DOI: 10.1186/s40645-020-0321-y (2020).

168. Erikson, L., Hegermiller, C., Barnard, P., Ruggiero, P. & van Ormondt, M. Projected wave conditions in the eastern north pacific under the influence of two cmip5 climate scenarios. *Ocean. Model.* **96**, 171–185, DOI: 10.1016/j.ocemod.2015.07.004 (2015).

169. Kumar, V. S. & Anand, N. M. Variations in wave direction estimated using first and second order Fourier coefficients. *Ocean. Eng.* **31**, 2105–2119, DOI: 10.1016/j.oceaneng.2004.06.003 (2004).

170. Sundar, V. Wave Characteristics Off the South east coast of India. *Ocean. engineering* **13**, 327–338 (1986).

171. Gowthaman, R. *et al.* Waves in Gulf of Mannar and Palk Bay around Dhanushkodi, Tamil Nadu, India. *Curr. Sci.* **104**, 1431–1435 (2013).

172. Kumar, V. S., Dubhashi, K. K. & Balakrishnan Nair, T. T. Spectral wave characteristics off Gangavaram, Bay of Bengal. *J. Oceanogr.* **70**, 307–321, DOI: 10.1007/s10872-014-0223-y (2014).

173. Kamranzad, B. Persian Gulf zone classification based on the wind and wave climate variability. *Ocean. Eng.* **169**, 604–635, DOI: 10.1016/j.oceaneng.2018.09.020 (2018).

174. Patra, A. & Bhaskaran, P. K. Trends in wind-wave climate over the head Bay of Bengal region. *Int. J. Climatol.* **36**, 4222–4240, DOI: 10.1002/joc.4627 (2016).

175. Patra, A. & Bhaskaran, P. K. Temporal variability in wind–wave climate and its validation with ESSO-NIOT wave atlas for the head Bay of Bengal. *Clim. Dyn.* **49**, 1271–1288, DOI: 10.1007/s00382-016-3385-z (2017).

176. Shanas, P. R. & Kumar, V. S. Trends in surface wind speed and significant wave height as revealed by ERA-Interim wind wave hindcast in the Central Bay of Bengal. *Int. J. Climatol.* **35**, 2654–2663 (2015).

177. Shanas, P. R., Aboobacker, V. M., Albarakati, A. M. & Zubier, K. M. Climate driven variability of wind-waves in the Red Sea. *Ocean. Model.* **119**, 105–117, DOI: 10.1016/j.ocemod.2017.10.001 (2017).

178. Anoop, T. R., Kumar, V. S., Shanas, P. R. & Johnson, G. Surface wave climatology and its variability in the north Indian Ocean Based on ERA-interim reanalysis. *J. Atmospheric Ocean. Technol.* **32**, 1372–1385, DOI: 10.1175/JTECH-D-14-00212.1 (2015).

179. Kumar, V. S. & Anoop, T. R. Spatial and temporal variations of wave height in shelf seas around India. *Nat. hazards* **78**, 1693–1706 (2015).

180. Shanas, P. R. & Kumar, V. S. Temporal variations in the wind and wave climate at a location in the eastern Arabian Sea based on ERA-Interim reanalysis data. *Nat. Hazards Earth Syst. Sci.* **14**, 1371–1381, DOI: 10.5194/nhess-14-1371-2014 (2014).

181. Gupta, N. & Bhaskaran, P. K. Inter-dependency of wave parameters and directional analysis of ocean wind-wave climate for the Indian Ocean. *Int. J. Climatol.* **37**, 3036–3043, DOI: 10.1002/joc.4898 (2016).

182. Hithin, N. K., Kumar, V. S. & Shanas, P. R. Trends of wave height and period in the Central Arabian Sea from 1996 to 2012: A study based on satellite altimeter data. *Ocean. Eng.* **108**, 416–425, DOI: 10.1016/j.oceaneng.2015.08.024 (2015).

183. Semedo, A., SušElj, K., Rutgersson, A. & Sterl, A. A global view on the wind sea and swell climate and variability from ERA-40. *J. Clim.* **24**, 1461–1479, DOI: 10.1175/2010JCLI3718.1 (2011).

184. Schott, F. A. & McCreary, J. P. The monsoon circulation of the Indian Ocean. *Prog. Oceanogr.* **51**, 1–123, DOI: 10.1016/S0079-6611(01)00083-0 (2001).

185. Kumar, P., Kaur, S., Weller, E. & Min, S.-K. Influence of Natural Climate Variability on the Extreme Ocean Surface Wave Heights Over the Indian Ocean. *J. Geophys. Res. Ocean.* **124**, 6176–6199, DOI: 10.1029/2019JC015391 (2019).

186. Young, I., Zieger, S. & Babanin, A. Global trends in wind speed and wave height. *Science* **332**, 451–455 (2011).

187. Takbash, A., Young, I. R. & Breivik, Ø. Global Wind Speed and Wave Height Extremes Derived from Long-Duration Satellite Records. *J. Clim.* **32**, 109–126, DOI: 10.1175/JCLI-D-18-0520.1 (2019).

188. Remya, P. G., Kumar, B. P., Srinivas, G. & Balakrishnan Nair, T. M. Impact of tropical and extra tropical climate variability on Indian Ocean surface waves. *Clim. Dyn.* **54**, 4919–4933, DOI: 10.1007/s00382-020-05262-x (2020).

189. Kumar, Prashant Min, S. K., Weller, E., Lee, H. & Wang, X. L. Influence of climate variability on extreme ocean surface wave heights assessed from ERA-interim and ERA-20C. *J. Clim.* **29**, 4031–4046, DOI: 10.1175/JCLI-D-15-0580.1 (2016).

190. Marshall, A. G., Hemer, M. A., Hendon, H. H. & McInnes, K. L. Southern annular mode impacts on global ocean surface waves. *Ocean. Model.* **129**, 58–74, DOI: 10.1016/j.ocemod.2018.07.007 (2018).

191. Patra, A., Min, S. K. & Seong, M. G. Climate Variability Impacts on Global Extreme Wave Heights: Seasonal Assessment Using Satellite Data and ERA5 Reanalysis. *J. Geophys. Res. Ocean.* **125**, e2020JC016754, DOI: 10.1029/2020JC016754 (2020).

192. Singh, O. P., Ali Khan, T. M. & Rahman, M. S. Probable reasons for enhanced cyclogenesis in the Bay of Bengal during July-August of ENSO years. *Glob. Planet. Chang.* **29**, 135–147, DOI: 10.1016/S0921-8181(00)00090-4 (2001).

193. Odériz, I. *et al.* Natural Variability and Warming Signals in Global Ocean Wave Climates. *Geophys. Res. Lett.* **48**, e2021GL093622, DOI: 10.1029/2021GL093622 (2021).

194. Reiter, E. R. The interannual variability of the ocean-atmosphere system. *J. Atmospheric Sci.* **35**, 349–370 (1978).

195. Srinivas, G., Remya, P. G., Malavika, S. & Balakrishnan Nair, T. M. The influence of boreal summer intraseasonal oscillations on Indowestern Pacific Ocean surface waves. *Sci. Reports* **10**, 1–12, DOI: 10.1038/s41598-020-69496-9 (2020).

196. Anoop, T. R., Kumar, V. . S., Shanas, P. R., Glejin, J. & Amrutha, M. M. Indian Ocean Dipole modulated wave climate of eastern Arabian Sea. *Ocean. Sci.* **12**, 369–378, DOI: 10.5194/os-12-369-2016 (2016).

197. Marshall, A., Hendon, H., Durrant, T. & Hemer, M. Madden julian oscillation impacts on global ocean surface waves. *Ocean. Model.* **96** (2015).

198. Dobrynin, M., Murawsky, J. & Yang, S. Evolution of the global wind wave climate in CMIP5 experiments. *Geophys. Res. Lett.* **39**, L18606, DOI: 10.1029/2012GL052843 (2012).

199. Fan, Y., Lin, S.-J., Griffies, S. & Hemer, M. Simulated global swell and wind-sea climate and their responses to anthropogenic climate change at the end of the twenty-first century. *J. Clim.* **27** (2014).

200. O'Grady, J. G., Hemer, M. A., McInnes, K. L., Trenham, C. E. & Stephenson, A. G. Projected incremental changes to extreme wind-driven wave heights for the twenty-first century. *Sci. Reports* **11**, DOI: 10.1038/s41598-021-87358-w (2021).

201. Kamranzad, B. & Mori, N. Future wind and wave climate projections in the Indian Ocean based on a super-high-resolution MRI-AGCM3.2S model projection. *Clim. Dyn.* **53**, 2391–2410, DOI: 10.1007/s00382-019-04861-7 (2019).

202. Roshin, E. & Deo, M. C. Derivation of design waves along the Indian coastline incorporating climate change. *J. Mar. Sci. Technol. (Japan)* **22**, 61–70, DOI: 10.1007/s00773-016-0393-y (2017).

203. Alizadeh, M. J., Alinejad-Tabrizi, T., Kavianpour, M. R. & Shamshirband, S. Projection of spatiotemporal variability of wave power in the Persian Gulf by the end of 21st century: GCM and CORDEX ensemble. *J. Clean. Prod.* **256**, 120400, DOI: https://doi.org/10.1016/j.jclepro.2020.120400 (2020).

204. Kamranzad, B., Etemad-Shahidi, A., Chegini, V. & Yeganeh-Bakhtiary, A. Climate change impact on wave energy in the Persian Gulf. *Ocean. Dyn.* **65**, 777–794, DOI: 10.1007/s10236-015-0833-y (2015).

205. Wandres, M., Pattiaratchi, C. & Hemer, M. Projected changes of the southwest australian wave climate under two atmospheric greenhouse gas concetration pathways. *Ocean. Model.* **117**, 9 (2017).

206. Semedo, A. *et al.* The wind sea and swell waves climate in the Nordic seas. *Ocean. Dyn.* **65**, 223–240, DOI: 10.1007/S10236-014-0788-4/TABLES/1 (2015).

207. Stopa, J., Ardhuin, F. & Girard-Ardhuin, F. Wave climate in the arctic 1992-2014: seasonality and trends. *The Cryosphere Discuss* 1–45 (2016).

208. Wang, X., Casas-Prat, M., Feng, Y., Crosby, A. & Swail, V. Historical changes in the davis strait baffin bay surface winds and waves, 1979–2016. *J. Clim.* **34**, 8879–8896 (2021).

209. Kohout, A. L., Williams, M. J., Dean, S. M. & Meylan, M. H. Storm-induced sea-ice breakup and the implications for ice extent. *Nat. 2014 509:7502* **509**, 604–607, DOI: 10.1038/nature13262 (2014).

210. Squire, V. Ocean wave interactions with sea ice: A reappraisal. *Annu. Rev. Fluid Mech.* **52**, 37–60, DOI: 10.1146/annurev-fluid-010719-060301 (2020).

211. Barnhart, K. R., Overeem, I. & Anderson, R. S. The effect of changing sea ice on the physical vulnerability of Arctic coasts. *Cryosphere* **8**, 1777–1799, DOI: 10.5194/TC-8-1777-2014 (2014).

212. Thomson, J. *et al.* .

213. Witze, A. Arctic sea ice hits second-lowest level on record. *Nature* DOI: 10.1038/d41586-020-02705-7 (2020).

214. Liu, Q., Babanin, A. V., Zieger, S., Young, I. R. & Guan, C. Wind and Wave Climate in the Arctic Ocean as Observed by Altimeters. *J. Clim.* **29**, 7957–7975, DOI: 10.1175/JCLI-D-16-0219.1 (2016).

215. Wang, X. L., Feng, Y., Swail, V. R. & Cox, A. Historical Changes in the Beaufort–Chukchi–Bering Seas Surface Winds and Waves, 1971–2013. *J. Clim.* **28**, 7457–7469, DOI: 10.1175/JCLI-D-15-0190.1 (2015).

216. Wang, X. L., Casas-Prat, M., Feng, Y., Crosby, A. & Swail, V. R. Historical Changes in the Davis Strait Baffin Bay Surface Winds and Waves, 1979–2016. *J. Clim.* **34**, 8879–8896, DOI: 10.1175/JCLI-D-21-0054.1 (2021).

217. Francis, O. P., Panteleev, G. G. & Atkinson, D. E. Ocean wave conditions in the Chukchi Sea from satellite and in situ observations. *Geophys. Res. Lett.* **38**, DOI: 10.1029/2011GL049839 (2011).

218. Thomson, J., Fan, Y., Stammerjohn, S., Stopa, J. & Rogers, E. Emerging trends in the sea state of the beaufort and chukchi seas. *Ocean. Model.* **105**, 1–12, DOI: 10.1016/j.ocemod.2016.02.009 (2016).

219. Waseda, T. *et al.* Correlated Increase of High Ocean Waves and Winds in the Ice-Free Waters of the Arctic Ocean. *Sci. Reports 2018 8:1* **8**, 1–9, DOI: 10.1038/s41598-018-22500-9 (2018).

220. Bush, E. & Lemmen, D. Canada's Changing Climate Report. Tech. Rep., Government of Canada, Ottawa, ON (2019).

221. Moore, G. W., Schweiger, A., Zhang, J. & Steele, M. Collapse of the 2017 Winter Beaufort High: A Response to Thinning Sea Ice? *Geophys. Res. Lett.* **45**, 2860–2869, DOI: 10.1002/2017GL076446 (2018).

222. Jansen, E. *et al.* Past perspectives on the present era of abrupt arctic climate change. *Nat. Clim. Chang.* **10**, 714–721, DOI: 10.1038/s41558-020-0860-7 (2020).

223. Rantanen, M. *et al.* The arctic has warmed nearly four times faster than the globe since 1979. *Nat. Commun. Earth Environ.* **3**, 168, DOI: 10.1038/s43247-022-00498-3 (2022).

224. Jenkins, M. & Dai, A. The Impact of Sea-Ice Loss on Arctic Climate Feedbacks and Their Role for Arctic Amplification. *Geophys. Res. Lett.* **48**, e2021GL094599, DOI: 10.1029/2021GL094599 (2021).

225. Batenson, A. Impact of sea ice floe size distribution on seasonal fragmentation and melt of arctic sea ice. *Cryosphere* **14**, 403–428 (2020).

226. Mioduszewski, J., Vavrus, S. & Wang, M. Arctic sea ice promotes stronger surface winds. *J. Clim.* **31**, 8101–8119, DOI: 10.1175/JCLI-D-18-0109.1 (2018).

227. Notz, D. & Community, S. Arctic Sea Ice in CMIP6. *Geophys. Res. Lett.* **47**, e2019GL086749, DOI: 10.1029/2019GL086749 (2020).

228. Shen, Z., Duan, A., Li, D. & Li, J. Assessment and Ranking of Climate Models in Arctic Sea Ice Cover Simulation: From CMIP5 to CMIP6. *J. Clim.* **34**, 3609–3627, DOI: 10.1175/JCLI-D-20-0294.1 (2021).

229. Perrie, W., Meylan, M., Toulany, B. & Casey, M. Modelling wave–ice interactions in three dimensions in the marginal ice zone. *Philos. Transactions R. Soc. A* **380**, 20210263, DOI: 10.1098/rsta.2021.0263 (2022).

230. Stopa, J. E., Sutherland, P. & Ardhuin, F. Strong and highly variable push of ocean waves on Southern Ocean sea ice. *Proc. Natl. Acad. Sci. United States Am.* **115**, 5861–5865, DOI: 10.1073/PNAS.1802011115/-/DCSUPPLEMENTAL (2018).

231. Theron, A. *et al.* Quantification of risks to coastal areas and development: wave run-up and erosion. In *CSIR 3rd Biennial Conference 2010. Science Real and Relevant,*, 16 (CSIR, CSIR International Convention Centre, Pertoria, 2010).

232. Martínez, C. *et al.* Coastal erosion in central Chile: A new hazard? *Ocean. & Coast. Manag.* **156**, 141–155, DOI: 10.1016/J.OCECOAMAN.2017.07.011 (2018).

233. Meucci, A., Young, I. R. & Breivik, Ø. Wind and Wave Extremes from Atmosphere and Wave Model Ensembles. *J. Clim.* **31**, 8819–8842, DOI: 10.1175/JCLI-D-18-0217.1 (2018).

234. Young, I. & Donelan, M. On the determination of global ocean wind and wave climate from satellite observations. *Remote. sensing Environ.* **215**, 228–241 (2018).

235. Takbash, A. & Young, I. R. Global ocean extreme wave heights from spatial ensemble data. *J. Clim.* **32**, 6823–6836, DOI: 10.1175/JCLI-D-19-0255.1 (2019).

236. Hande, L. B., Siems, S. T. & Manton, M. J. Observed Trends in Wind Speed over the Southern Ocean. *Geophys. Res. Lett.* **39**, 11802, DOI: 10.1029/2012GL051734 (2012).

237. Thompson And, D. W. J. & Wallace, J. M. Annular Modes in the Extratropical Circulation. Part I: Month-to-Month Variability. *J. Clim.* **13**, 1000–1016, DOI: 10.1175/1520-0442(2000)013 (2000).

238. Trenberth, K. E. Interannual Variability of the 500 mb Zonal Mean Flow in the Southern Hemisphere in: Monthly Weather Review Volume 107 Issue 11 (1979). *Mon. Weather. Rev.* **107**, 1515–1524 (1979).

239. Fyfe, J. C. Extratropical Southern Hemisphere Cyclones: Harbingers of Climate Change? in: Journal of Climate Volume 16 Issue 17 (2003). *J. Clim.* **16**, 2802–2805 (2003).

240. Masselink, G. *et al.* Extreme wave activity during 2013/2014 winter and morphological impacts along the Atlantic coast of Europe. *Geophys. Res. Lett.* **43**, 2135–2143, DOI: 10.1002/2015GL067492 (2016).

241. Castelle, B. *et al.* Impact of the winter 2013–2014 series of severe Western Europe storms on a double-barred sandy coast: Beach and dune erosion and megacusp embayments. *Geomorphology* **238**, 135–148, DOI: 10.1016/J.GEOMORPH.2015.03.006 (2015).

242. Earlie, C. S., Young, A. P., Masselink, G. & Russell, P. E. Coastal cliff ground motions and response to extreme storm waves. *Geophys. Res. Lett.* **42**, 847–854, DOI: 10.1002/2014GL062534 (2015).

243. Dodet, G., Bertin, X. & Taborda, R. Wave climate variability in the north-east atlantic ocean over the last six decades. *Ocean. Model.* **31**, 120–131 (2010).

244. Vousdoukas, M. I. & et al. Global probabilistic projections of extreme sea levels show intensification of coastal flood hazard. *Nat. Commun.* **9** (2018).

245. Yang, S. & Oh, J. H. Effects of modes of climate variability on wave power during boreal summer in the western North Pacific. *Sci. Reports 2020 10:1* **10**, 1–10, DOI: 10.1038/s41598-020-62138-0 (2020).

246. Hoeke, R. K. *et al.* Widespread inundation of Pacific islands triggered by distant-source wind-waves. *Glob. Planet. Chang.* **108**, 128–138, DOI: 10.1016/J.GLOPLACHA.2013.06.006 (2013).

247. Storlazzi, C. & et al. Most atolls will be uninhabitable by the mid-21st century because of sea-level rise exacerbating wave-driven flooding. *Sci. Adv.* **4** (2018).

248. Amores, A. *et al.* Coastal Flooding in the Maldives Induced by Mean Sea-Level Rise and Wind-Waves: From Global to Local Coastal Modelling. *Front. Mar. Sci.* **8**, 705, DOI: 10.3389/FMARS.2021.665672/BIBTEX (2021).

249. Wadey, M., Brown, S., Nicholls, R. J. & Haigh, I. Coastal flooding in the Maldives: an assessment of historic events and their implications. *Nat. Hazards* **89**, 131–159, DOI: 10.1007/S11069-017-2957-5/FIGURES/9 (2017).

250. Amores, A., Marcos, M., Le Cozannet, G. & Hinkel, J. Coastal flooding and mean sea-level rise allowances in atoll island. *Sci. Reports* **12**, DOI: 10.1038/s41598-022-05329-1 (2022).

251. Mori, N. & Shimura, T. Tropical cyclone-induced coastal sea level projection and the adaptation to a changing climate. *Camb. Prisms* (2023).

252. Mori, N. & Takemi, T. Impact assessment of coastal hazards due to future changes of tropical cyclones in the north pacific ocean. *Weather. Clim. Extrem.* **11**, 53–69, DOI: 10.1016/j.wace.2015.09.002 (2016).

253. Suh, K.-D., Kim, S.-W., Mori, N. & Mase, H. Effect of climate change on performance-based design of caisson breakwaters. *J. waterway, port, coastal ocean engineering* **138**, 3 (2012).

254. Bisoi, S. & Haldar, S. Impact of climate change on dynamic behavior of offshore wind turbine. *Mar. Georesources Geotechnol.* **35**, 905–920, DOI: 10.1080/1064119X.2016.1257671 (2017).

255. Atkinson, D. E. Observed storminess patterns and trends in the circum-arctic coastal regime. *Geo-Marine Lett.* **25**, 98–109 (2005).

256. Irrgang, A. M., Lantuit, H., Manson, G. K. & G}u. .

257. Gudmestad, O. The changing climate and the arctic coastal settlements. **1**, 411–419 (2018).

258. Melvin, A. M. *et al.* Climate change damages to Alaska public infrastructure and the economics of proactive adaptation. *Proc. Natl. Acad. Sci. United States Am.* **114**, E122–E131, DOI: 10.1073/PNAS.1611056113/-/DCSUPPLEMENTAL (2017).

259. Radosavljevic, B. & et al. Threats to coastal infrastructure in the arctic: A case study from herschel island, yukon territory, canada. *Estuaries Coasts* **39**, 900–915 (2016).

260. Houghton, I., Hegermiller, C., Teicheira, C. & Smit, P. Operational assimilation of spectral wave data from the sofar spotter network. *Geophys. Res. Lett.* **49**, e2022GL098973, DOI: 10.1029/2022GL098973 (2022).

261. Greenslade, D. & et al. 15 priorities for wind-wave research: An australian perspective. *Bull. Am. Meteorol. Soc.* **101**, E446–E461, DOI: 10.1175/BAMS-D-18-0262.1 (2020).

262. Wang, X. Accounting for autocorrelation in detecting mean-shifts in climate date series using the penalized maximal t or f test. *J. Appl. Meteorol. Climatol.* **47**, 2493–2444 (2008).

263. Dullaart, J. & et al. Accounting for tropical cyclones more than doubles the global population exposed to low-probability coastal flooding. *Commun. Earth Environ.* **2**, DOI: 10.1038/s43247-021-00204-9 (2021).

264. Kattsov, V. & et al. Arctic sea-ice change: a grand challenge of climate science. *J. Glaciol.* **56**, 1115–1121, DOI: 10.3189/002214311796406176 (2017).

265. Watts, M. & et al. A spatial evaluation of arctic sea ice and regional limitations in cmip6 historical simulations. *J. Clim.* **34**, 6399–6400, DOI: 10.1175/JCLI-D-20-0491.1 (2021).

266. Cavaleri, L., Barbariol, F. & Benetazzo, A. Wind-wave modeling: where we are, where to go. *J. marine science engineering* **260**, DOI: 10.3390/jmse8040260 (2020).

267. Babanin, A. Ocean waves in large-scale air-sea weather and climate systems. *J. Geophys. Res. Ocean.* **128**, e2023JC019633, DOI: 10.1029/2023JC019633 (2023).

268. Gemmrich, J. & Cicon, L. Generation mechanism and prediction of an observed extreme rogue wave. *Nat. Sci. Reports* **12**, DOI: 10.1038/s41598-022-05671-4 (2022).

269. Blockey, E. & et al. The future of sea ice modeling: where do we go from here? *Bull. Am. Meteorol. Soc.* **101**, E1304–E1311, DOI: https://doi.org/10.1175/BAMS-D-20-0073.1 (2020).

270. Chen, J., Pillai, A., Johanning, L. & Ashton, I. Using machine learning to derive spatial wave data: a case study for a marine energy site. *Environ. modelling software* **142**, 105066 (2021).

271. Antolínez, J. *et al.* Downscaling changing coastlines in a changing climate: the hybrid approach. *J. Geophys. Res. Ocean.* **123**, 229–251, DOI: 10.1002/2017JF004367 (2018).

272. Ricondo, A. *et al.* Hywaves: Hybrid downscaling of multimodal wave spectra to nearshore areas. *Ocean. Model.* **184**, 102210, DOI: 10.1016/j.ocemod.2023.102210 (2023).

273. J.B., S., Erikson, L. & Barnard, P. Characterizing storm-induced coastal change hazards along the united states west coast. *Nat. Sci. Data* **9**, DOI: 10.1038/s41597-022-01313-6 (2022).

274. Zimmermann, M. *et al.* Nearshore bathymetric changes along the alaska beaufort sea coast and possible physical drivers. *Cont. Shelf Res.* **242**, 104742, DOI: 10.1016/j.csr.2022.104745 (2022).

275. Cavaleri & et al. Wave modelling in coastal and inner seas. *Prog. Oceanogr.* **167**, 164–233, DOI: 10.1016/j.pocean.2018.03.010 (2018).

276. Diex-Sierra, J. & et al. The worlwide c3s cordex grand ensemble: a major contribution to assess regional climate change in the ipcc ar6 atlas. *Bull. Am. Meteorol. Soc.* **103**, E2804–E2826, DOI: 10.1175/BAMS-D-22-0111.1 (2022).

277. Marcos, M. *et al.* Increased extreme coastal water levels due to the combined action of storm surges and wind waves. *Geophys. Res. Lett.* **46**, 4356–4364, DOI: 10.1029/2019GL082599 (2019).

278. Santos, V. *et al.* Statistical modelling and climate variability of compound surge and precipitation events in a managed water system: a case study in the netherlands. *Hydrol. Earth Syst. Sci.* **25**, 3595–3615 (2021).

279. Zscheischler, J. & et al. Future climate risk from compound events. *Nat. Clim. Chang.* **8**, 469–477 (2018).

280. Zscheischler, J. & et al. A typology of compound weather and climate events. *Nat. Rev. Earth Environ.* **1**, 333–347 (2020).

281. Hongo, C., Kurihara, H. & Golbuu, Y. Projecting of wave height and water level on reef-lined coasts due to intensified tropical cyclones and sea level rise in palau to 2100. *Nat. Hazards Earth Syst. Sci.* **18**, 669–686, DOI: 10.5194/nhess-18-669-2018 (2018).

282. Callaghan, D., Mumby, P. & Mason, M. Near-reef and nearshore tropical cyclone wave climate in the great barrier reef with and without reef structure. *Coast. Eng.* **157**, 103652, DOI: 10.1016/j.coastaleng.2020.103652 (2020).

283. Ribal, A. & Young, I. 33 of globally calibrated wave height and wind speed data based on altimeter observations. *Nat. Sci. Data* **6**, 77, DOI: 10.1038/s41597-019-0083-9 (2019).

284. Ribal, A. & Young, I. 33 years of globally calibrated wave height and wind speed data based on altimeter observations. *Aust. Ocean. Data Netw.* DOI: 10.26198/5c77588b32cc1 (2019).

285. Piollé, J.-F., Dodet, G. & Quilfen, Y. ESA Sea State Climate Change Initiative: Global remote sensing merged multi-mission monthly gridded significant wave height, L4 product, version 1.1. *Centre for Environ. Data Analysis* DOI: 10.5285/47140d618dcc40309e1edbca7e773478 (2020).

286. Wang, X. & Swail, V. Changes of extreme wave heights in northern hemisphere oceans and related atmospheric circultion regimes. *J. Clim.* **14**, 2204–2221, DOI: 10.1175/1520-0442(2001)014<2204:COEWHI>2.0.CO;2 (2001).

287. Gutiérrez, J. & et al. *Atlas. In Climate Change 2021: The Physical Science Basis. Contribution of Working Group I to the Sixth Assessment Report of the Intergovernmental Panel on Climate Change [Masson-Delmotte, V., P. Zhai, A. Pirani, S.L. Connors, C. Péan, S. Berger, N. Caud, Y. Chen, L.Goldfarb, M.I. Gomis, M. Huang, K. Leitzell, E. Lonnoy, J.B.R. Matthews, T.K.Maycock, T. Waterfield, O. Yelekçi, R. Yu, and B. Zhou (eds.)].* (Cambridge University Press, 2021).

288. Tebaldi, C., Arblaster, J. & Knutti, R. Mapping model agreement on future climate projections. *Geophys. Res. Lett.* **38**, DOI: 10.1029/2011GL049863 (2011).

Acknowledgements

J.M. acknowledges the University of Central Florida (UCF) Pre-eminent program (P3).

Author contributions

M.C.-P. led the writing of the manuscript, conducted the majority of the analyses presented herein, and made Figs. 2-5, Table 1, and supplementary tables and figures. G.D. made Fig. 1. M.C-P., M.H., G.D., J.M., X.W., N.M., and I.Y. contributed to the general design of the manuscript, including text structure and figure conceptualization. Y.F. contributed to the statistical data analysis. All co-authors (except Y.F.) contributed to the literature review, writing of initial drafts regarding specific sections, and to editing the final draft. In particular, M.C.-P., L.E. and X.W. contributed to the initial version of the Arctic Ocean section, G.D., M.M., X.W., M.C.-P. and J.M. contributed to the initial version of the Atlantic Ocean section, B.K. and P.K. contributed to the initial version of the Indian Ocean section, N.M., J.M., and X.W. contributed to the initial version of the Pacific Ocean section, and I.Y. and M.H. contributed to the initial version of the Southern Ocean section.

Competing interests

The authors declare no competing interests.

Key points

- A growing number of ocean wave studies have been developed since 2010s leading to an increased understanding of the wind wave climate changes under global warming but important uncertainties remain.
- Historical trend analysis is challenging due to the presence of temporal inhomogeneities in historical products as a result of an increase of the number and type of assimilated data over time.
- Future wave projections are affected by a chain of uncertainty factors, including variability related to wave and climate models, emission scenarios, and (the poorly known) internal natural variability.
- Future wave projections reveal robust increases over the Southern Ocean and tropical South Pacific, with the Arctic Ocean experimenting the most dramatic changes.
- Resolving global warming effects on coastal wind-waves, in addition to other marine drivers, is key to understand the impact on our coasts, but requires a step-up in our observational and model capabilities.
- Multidisciplinary fundamental modelling research, sustained increase of observations, and larger ensembles are needed to reduce uncertainty in wave climate changes across multiple scales, including contribution to extreme sea-level change.

Tables

Table 1. **Regional summary of most relevant and robust features of the historical and future changes in wind-wave conditions at each major ocean basin.**

Region	Climatology	Historical change	Response to teleconnections	Future projections by 2100 (RCP8.5)
Atlantic Ocean	Latitudinal gradient of H_s Large seasonal & inter-annual variability (ExTNA) Larger T_m in ESA Fetch-limited waves in Med EW θ_m in ExTA turning WW in TA	$\uparrow\downarrow$ H_s (Decadal 0.5-3 cm/yr; NA) $\uparrow$ H_s (After 1990's: 0.5-3 cm/yr; WMed)	$\uparrow$ H_s (NENA) with NAO+, AO+ & SCAND+ $\uparrow$ H_s (WsTNA) with NAO- & AO- $\uparrow$ H_s (Med) with NAO-, EA- $\uparrow$ H_s (ENA) with SCAND+, EA+	$\downarrow$ H_s (<10%; NA & Med) $\downarrow$ T_m (<5%; NA & Med) $\circlearrowright\theta_m$ (<10°; TA & ExTA)
Pacific Ocean	Latitudinal gradient of H_s Complex multi-modal waves in TP & dominant swell in ESP EW θ_m in ExTP, turning EqW (ETP) & Ws (WTP)	$\downarrow$ H_s (< 1 cm/yr; NP, with exception of WNP & California coast) $\uparrow$ H_{sx} (0.5-1 cm/yr; SP)	Strong ENSO influence $\uparrow$ H_s (NEP, SWTP) with SOI- (El Niño) $\uparrow$ H_s (NEP) with PDO+ and PNA+	$\downarrow$ H_s (<10%, NP, NWTP) $\uparrow$ T_m (<5%, EP) $\circlearrowright\theta_m$ (5°;10°; sTP & TP) $\circlearrowleft\theta_m$ (5°;10°; ExTP)
Indian Ocean	Poleward positive gradient of H_s SO swell affects NIO & SIO Strong influence of monsoon winds (NIO), which reverse direction annually EW θ_m (ExTI), & Eqw/SW in summer/winter (NIO)	$\uparrow$ $H_{s\mathrm{DJF}}$ (reg. average 0.4 cm/yr; IO) $\uparrow$ H_{sxDJF} (reg. average 0.6 cm/yr; IO) $\uparrow$ H_{sx} (>1 cm/yr; SIO)	$\uparrow$ H_s (BoB) during summer monoon & El Niño $\uparrow$ H_s (SIO) with SAM+	$\uparrow$ H_s (<10%; NIO, WTIO, all seasons except DJF) $\uparrow$ T_m (<5%) $\circlearrowleft\theta_m$ (<5°; WI)
Arctic Ocean	Historically limited wave influence in IA (semi-enclosed seas) & strong seasonal variability EA influenced by NA waves with Nw θ_m	Emergence of swell & $\uparrow$ H_s (1-3 cm/year, IA) $\uparrow$ H_{sx} (<10 cm/yr, particularly autumn) Unprecedented H_s >5 m (BS) in 2015 SIC reduction (with unprecedented minimum in 2012) is a key driver	$\uparrow$ H_s (NS, GS) with AO+, NAO+, and SCAND- Weakening of the normally anticyclonic climate (IA) linked to intrusion of NA waves when favored by SIC decline	Climate change hotspot with virtually ice-free Arctic by 2050 $\uparrow$ H_sT_m (<400%), particularly Jul-Nov above 70°N $\circlearrowleft\theta_m$ (BS)
Southern Ocean	Long fetches with sustained year-round intense waves Generation source of swells influencing PO, AO, IO	$\uparrow$ H_s (1-3 cm/yr)	$\uparrow$ H_s & $\uparrow$ Swell with SAM+, AAO+.	$\uparrow$ H_s (~5%) $\uparrow$ T_m (~5%) $\circlearrowleft\theta_m$ (3°- 5°)

NA, North Atlantic; ExTNA, Extra-tropical North Atlantic; ESA, Eastern South Atlantic; Med, Mediterranean Sea; ExTA, Extra-tropical Atlantic Ocean; WMed, Western Mediterranean Sea; NENA, Northeastern North Atlantic Ocean; WsTNA, Western sub-tropical North Atlantic Ocean; ENA, Eastern North Atlantic; TA, Tropical Atlantic; TP, Tropical Pacific; ESP, Eastern South Pacific; ExTP, Extra-tropical Pacific; ETP, Eastern Tropical Pacific; WTP, Western Tropical Pacific; NP, North Pacific; WNP, Western North Pacific; NEP, Northeastern Pacific; SWTP, Southwestern Tropical Pacific; NWTP, Northwestern Tropical Pacific; EP, Eastern Pacific; sTP,sub-Tropical Pacific; SO; Southern Ocean; NIO, North Indian Ocean; SIO, South Indian Ocean; ExTIO, Extra-tropical Indian Ocean; IO; Indian Ocean; BoB, Bay of Bengal; WTIO, Western Tropical Indian Ocean; WIO: Western Indian Ocean; IA; Inner Arctic; EA, Eastern Arctic; BS, Beaufort Sea; NS, Norwegian Sea; GS, Greenland Sea; PO, Pacific Ocean, AO, Atlantic Ocean; EW, Eastwards; WW, Westwards; EqW, Equator-wards; SW, Southwards; SIC, Sea ice cover; DJF, December-January-February. Unless otherwise stated, historical and projected changes refer to mean climatological values, and trends are specified for the 1980s to 2010s period. H_{sx} indicates high-frequency H_s extremes.

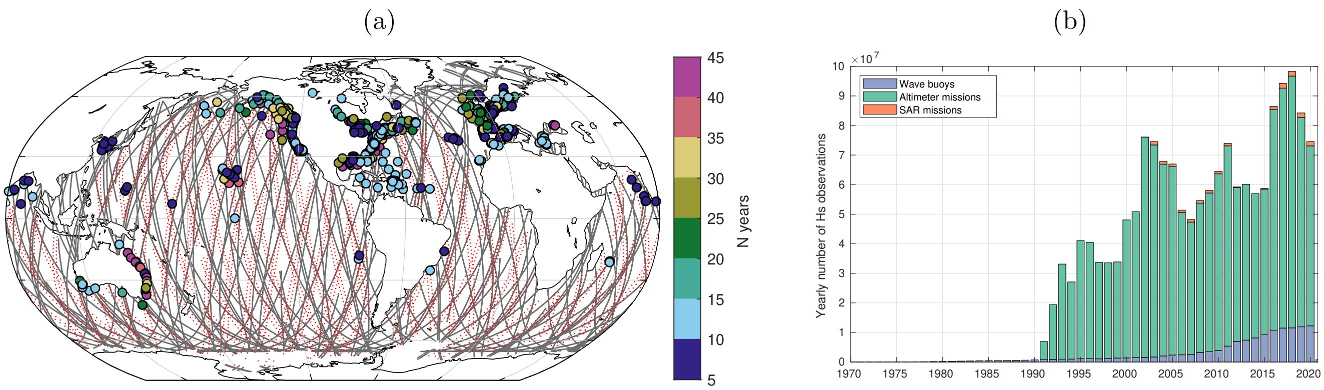

Figure 1. Spatial coverage and temporal evolution of H_s observations (a) Spatial sampling of wave buoys (colored circles) and one-day satellite acquisition of altimeter (grey line) and Synthetic aperture radar (SAR) missions (red dotted line). (b) Temporal evolution of the yearly number of significant wave height (H_s) observations from 1970 to 2020, including wave buoys (from the Copernicus Marine Service In Situ Thematic Center, available at https://marine.copernicus.eu/about/producers/insitu-tac), altimeter and SAR missions (from the ESA Sea State CCI database collection, available at https://catalogue.ceda.ac.uk/uuid/7cfcd20428c3454fafa4e1afec2cf92). Buoy sampling rate is comprised between 1-360 min (with over 70% buoys having either 30 or 60 min sampling rate), altimeter sampling rate is 1 Hz (corresponding to $\sim$ 7km spacing), and SAR sampling rate is $\sim$ 15 s (corresponding to $\sim$ 100km spacing). Only buoys with more than 5 years of records are shown. Altimeter missions include ERS-1, TOPEX, ERS-2, GFO, Jason-1, ENVISAT, Jason-2, Cryosat-2, SARAL, Jason-3 and Sentinel-3A. SAR missions include ENVISAT, Sentinel-1A and Sentinel-1B. Note that for the one-day example tracks shown in (a) only Jason-2, Cryosat-2 SARAL, Jason-3, Sentinel-3A, Sentinel-1A and Sentinel-1B are included. This figure illustrates the heterogeneous spatial coverage of moored buoys (with a larger density in the North Hemisphere), the limited time coverage of moored buoys (the large majority of buoys have only been operative for the last 20 years or less while only few buoys (violet) have been operative for more than 40 years), the near-global coverage of satellite acquisitions with a lower time resolution, and the notable increase of yearly number of wave observations over the last decades, with a big jump in the 1990s thanks to the contribution of satellite missions.

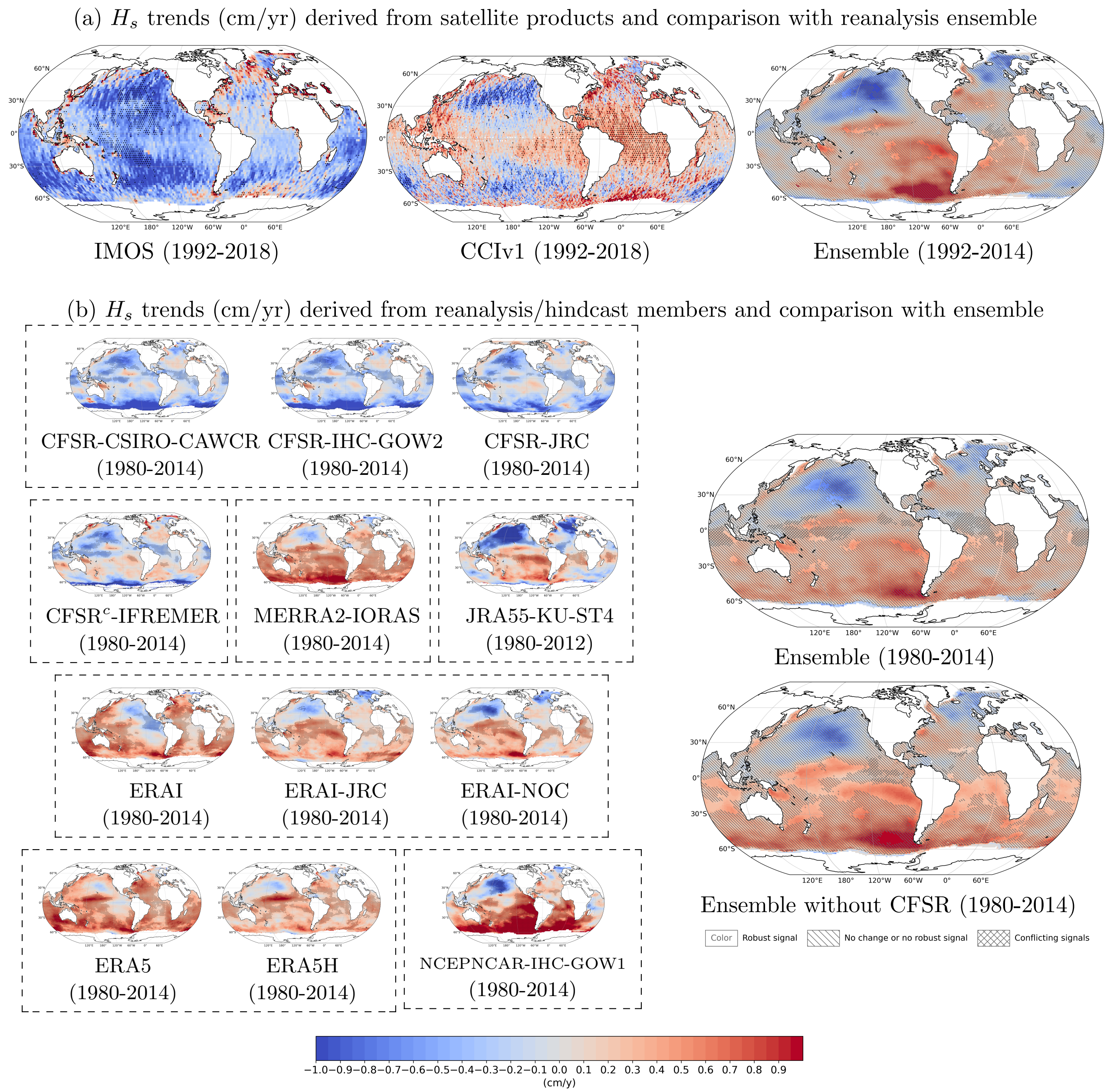

Figure 2. Historical H_s trend and discrepancies among data products. Annual mean significant wave height (H_s) trend (cm/yr) calculated over the indicated periods from (a) altimetry data (in comparison to reanalysis/hindcast ensemble average), and (b) individual ensemble members (in comparison with corresponding ensemble with and without CFSR-derived products). Results are derived from the IMOS global merged multi-mission monthly gridded altimetry dataset[283,284], the ESA CCI L4 product v1.1[285], and a global ensemble of ocean wave climate statistics from contemporary wave reanalysis and hindcasts[31] (see Table S1). The trend is computed with Sen's slope estimator in conjunction with a modified Mann-Kendall method that accounts for the effect of lag-1 autocorrelation by iterative pre-whitening[55,286]. Stippling indicates statistical significance of trends derived from individual products. Robustness and uncertainty in the ensemble averages is displayed as in the IPCC AR6 Interactive Atlas[287] with robust signal (no hatching) being defined as $>$ 50% models show statistically significant trend and 80% of those models agree on sign of change[288]. The ensemble average is weighted average so each driving atmospheric model has equal contribution. This figure illustrates the challenge in assessing trends due to the discrepancies among modern wave reanalyses/hindcasts and alimetry data, which relates to the presence of temporal inhomogeneities caused by the increase of observations overtime, and calibration differences.

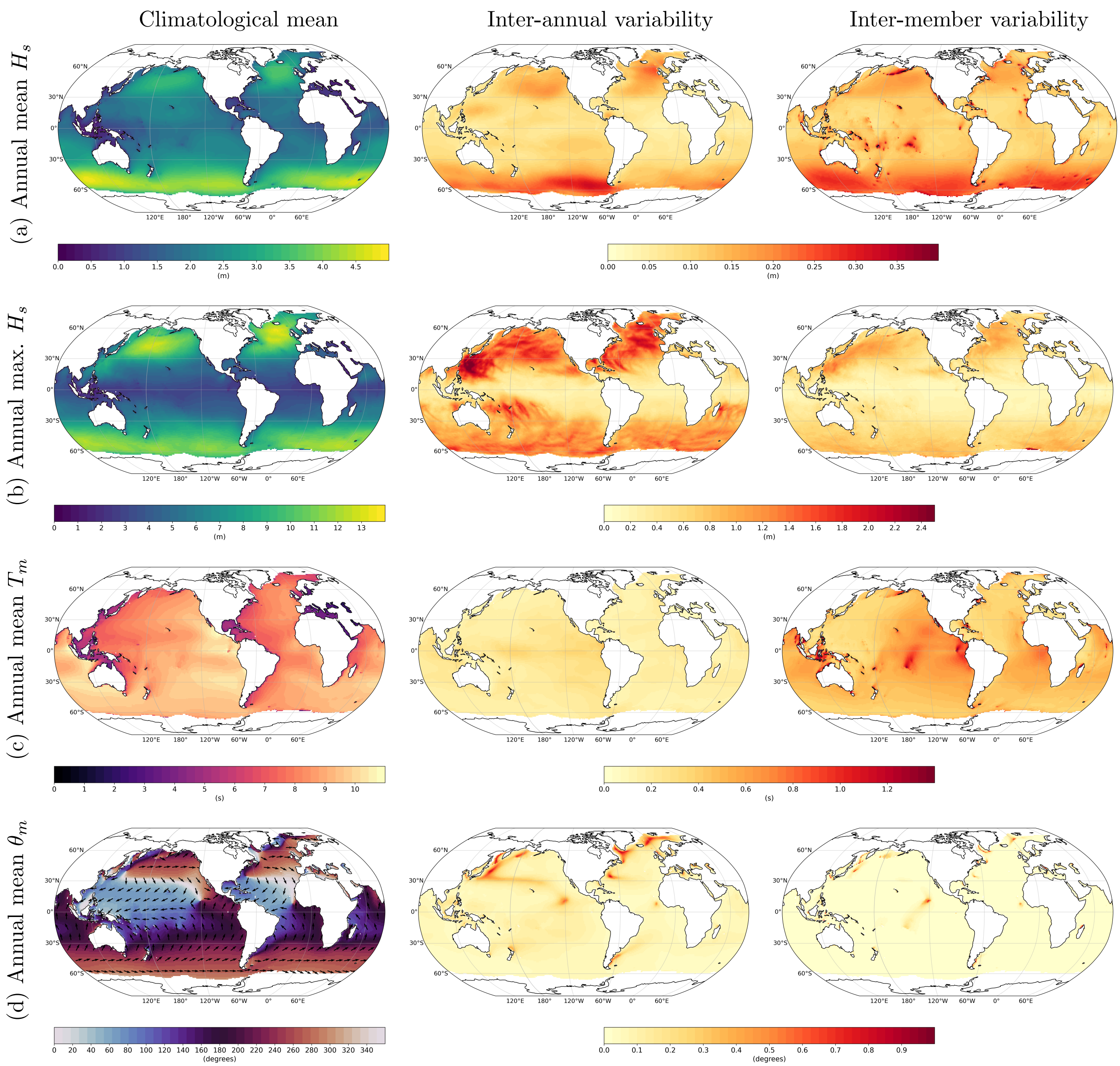

Figure 3. Historical climatology and variability of wind-waves. (a) Ensemble average of the historical climatological mean of the annual mean significant wave height (H_s) (m) (left panel), the ensemble average of its inter-annual variability (centre panel), and the corresponding inter-member variability (right panel). (b) As in panel (a) but annual maximum H_s (m). (c) As in panel (a) but annual mean T_m (s). (d) As in panel (a) but annual mean θ_m (°, nautical convention). Results are derived from a global ensemble of ocean wave climate statistics from contemporary wave reanalysis and hindcasts[31] that covers 1980–2014, with the exception of one ensemble member that covers 1980–2012 (see Table S1). CFSR-IFREMER T_m was not considered due the different T_m formulation (see Figure S4). The ensemble average is weighted average so each driving atmospheric model has equal contribution. The inter-annual variability is described as the ensemble average of the standard deviation of the corresponding annual values. The inter-member variability is described as the standard deviation of the corresponding climatological means of all members. This figure illustrates large-scale wind-wave features, such as energetic sea states in the mid-to-high latitudes and swell-dominated long waves in the Southern Ocean and the Eastern side of large basins, while it highlights regional uncertainty due to inter-member variability.

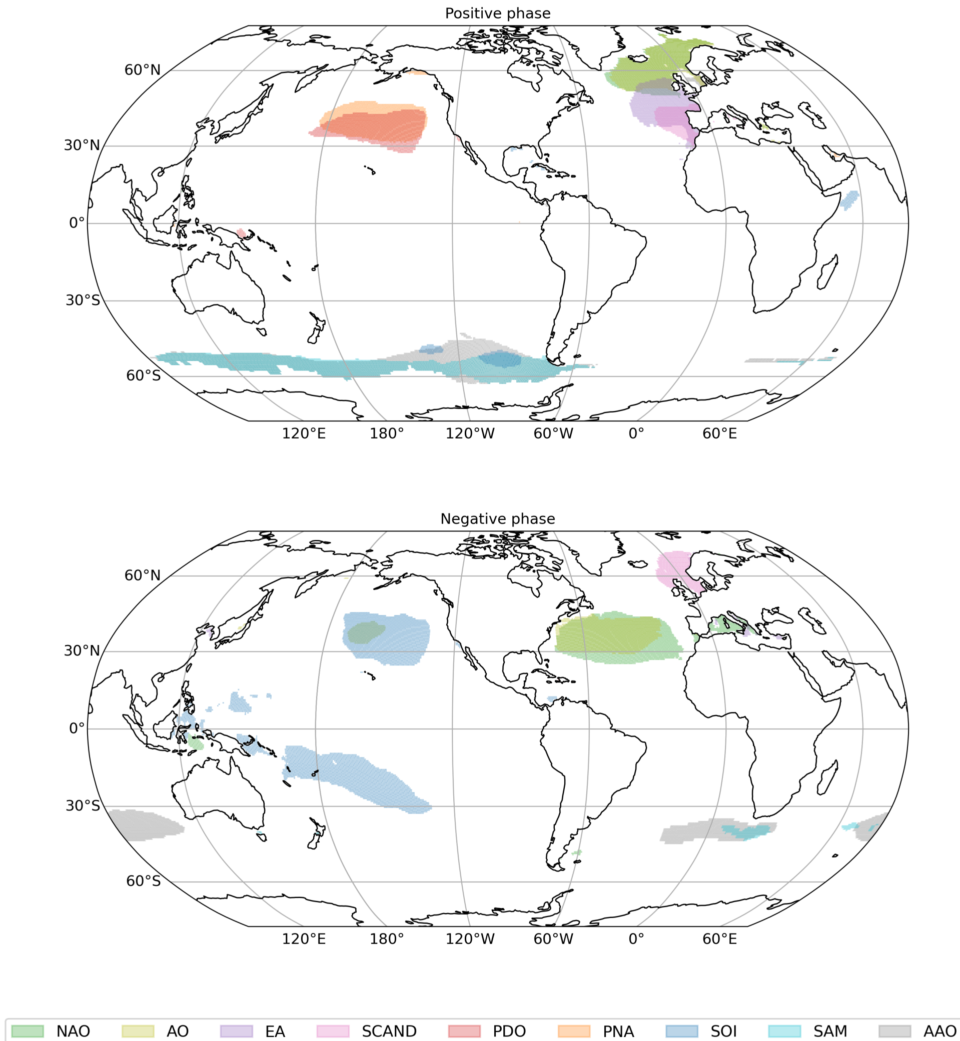

Figure 4. Areas of increased H_s during positive or negative phase of the indicated teleconnection pattern. Results are derived from a global ensemble of ocean wave climate statistics from contemporary wave reanalysis and hindcasts[31] that covers 1980–2014, with the exception of one ensemble member that covers 1980–2012 (see Figs. S12-S13 and Table S1). It also considers the North Atlantic Oscillation (NAO) index, the Arctic Oscillation (AO) index, the East Atlantic (EA) index, the Scandinavian (SCAND) index, the Southern Oscillation Index (SOI), the Pacific Decadal Oscillation (PDF) index, the Pacific North American (PNA) index, the Southern Annular Mode (SAM) Index, and the Antarctic Oscillation (AAO) index. Sustained large negative values of the SOI indicate an El Niño, positive values indicate (La Niña). The periods of positive (negative) phase are defined as the months when the corresponding teleconnection pattern standardized index is positive (negative) and exceeds one standard deviation in absolute value. Areas of increased wave height are identified where 80% of the ensemble members exhibit an averaged monthly mean H_s over the months of, respectively, positive and negative phases of the corresponding teleconnection pattern, that is at least 5% larger than the average of the climatological monthly mean H_s values. This figure illustrates large-scale atmospheric teleconnection patterns have an influence on wind-waves.

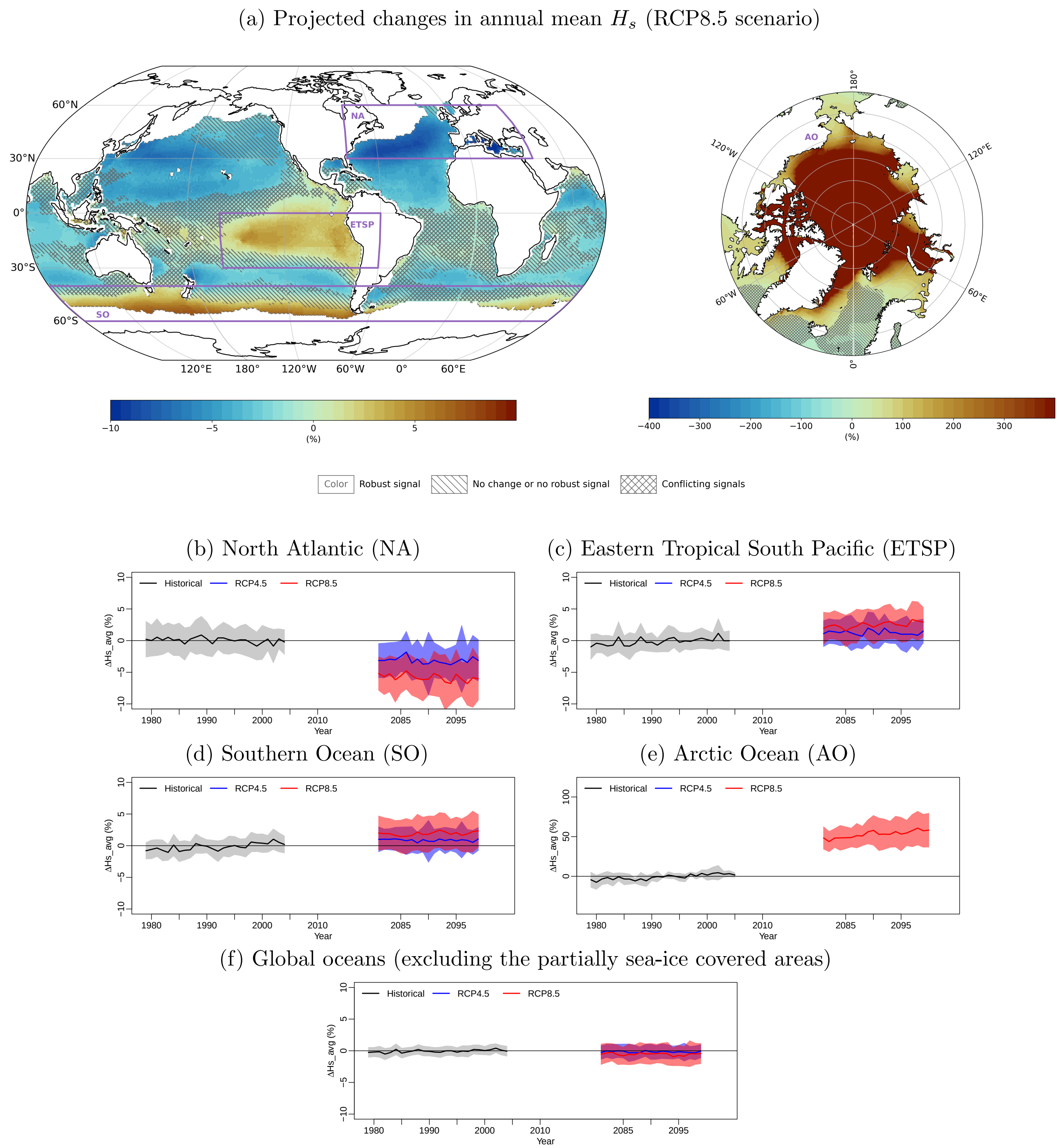

Figure 5. Future projected changes in H_s. (a) The ensemble average of the future (2081-2099) projected change of the climatological mean of the annual mean significant wave height (H_s) (m) for the RCP8.5 scenario, relative to the climatological mean of the historical period (1979-2004). Robustness and uncertainty is displayed as in the IPCC AR6 Interactive Atlas[287] with robust signal being defined as > 50% models show statistically significant change and 80% of these models agree on sign of change[288]. (b-f) Evolution of the regional average (over the indicated areas) of the yearly annual mean H_s (m) relative to the corresponding climatological mean of the historical period (1979-2004) (%), including RCP4.5 and RCP8.5 scenarios. Results (except for the Arctic Ocean) are derived from the latest global ensemble of ocean wave climate projections from CMIP5-driven models[36]. Results relative to the Arctic Ocean are derived from CMIP5-driven 5-member ensemble[95]. For each year in the regional panels (b-f), the inter-member variability is described as the standard deviation of the corresponding relative projected change for all members of the historical period (black), RCP4.5 scenario (blue), RCP8.5 scenario (red). This figure illustrates global H_s has no clear sign of increase or decrease but some regions exhibit a decrease or increase up to 10% (larger for RCP8.5 than for RCP4.5), except for the Arctic Ocean where relative changes are remarkably larger (note the change in scale).

Box 1 | Description of wind-waves

Wind-waves are only one type amongst a variety of waves that occur in the oceans, being typically shorter than 30 s and longer than 1/4 s[2]. As with many other types of waves, they can generally be described by their wave height (H), wave period (T), and wave direction (θ). However, the definition of wave height, or wave period, is non-trivial as the the sea state typically results from the combination of many harmonic wave components with different amplitudes, periods (or frequencies, f), phases and directions, that can be described by a 3D variance density wave spectrum[2] ($E(f,\theta)$), which can be simplified by a 2D spectrum by integrating over all directions ($E(f)$). For practical purposes, we often use spectrum-averaged (or derived) wave parameters to describe wind waves, being the most commonly used the significant wave height H_s, the mean(peak) wave period T_m (T_p) and the mean(peak) wave direction θ_m (θ_p).

H_s is a well-defined and standardized statistic to describe the characteristic wave height of the sea state, which is defined as the average height of the highest one-third of waves. It is largely used in coastal, naval, and offshore engineering, being one of the reasons for its widespread use the fact that H_s correlates fairly well with the wave height as historically estimated by experienced observers[2]. T_m, T_p, θ_m, and θ_p are also relevant spectrum-derived wave statistics that are widely used by researchers and engineers. T_m and θ_m are obtained from integrating the spectrum, while T_p and θ_p focus on the predominant (most energetic) wave system. These wave parameters are relevant metrics that have been, and continue to be, used to monitor changes in wave conditions, and assess their impacts. For example, high and steep waves (large H_s/L, where L is the wavelength and a function of T_m) have a larger potential for beach erosion, and infrastructure damage[22], while swell-dominated sea states with large wave periods are a flooding hazard for low-lying coastal areas[246]. T_m is also relevant for coastal and naval engineering as it can be linked to wave resonance and associated instability, while the combination of wave period and wave height ($H_s^2T_p$) translates into wave power. θ_m is a key feature affecting the long-shore sediment transport along coastal beaches, which can contribute to long-term coastal retreat. With increased accessibility to technology (storage and compute) and ability to analyse large and complex data, researchers are increasingly assessing characteristics of the full wave spectra over global scales.

2D

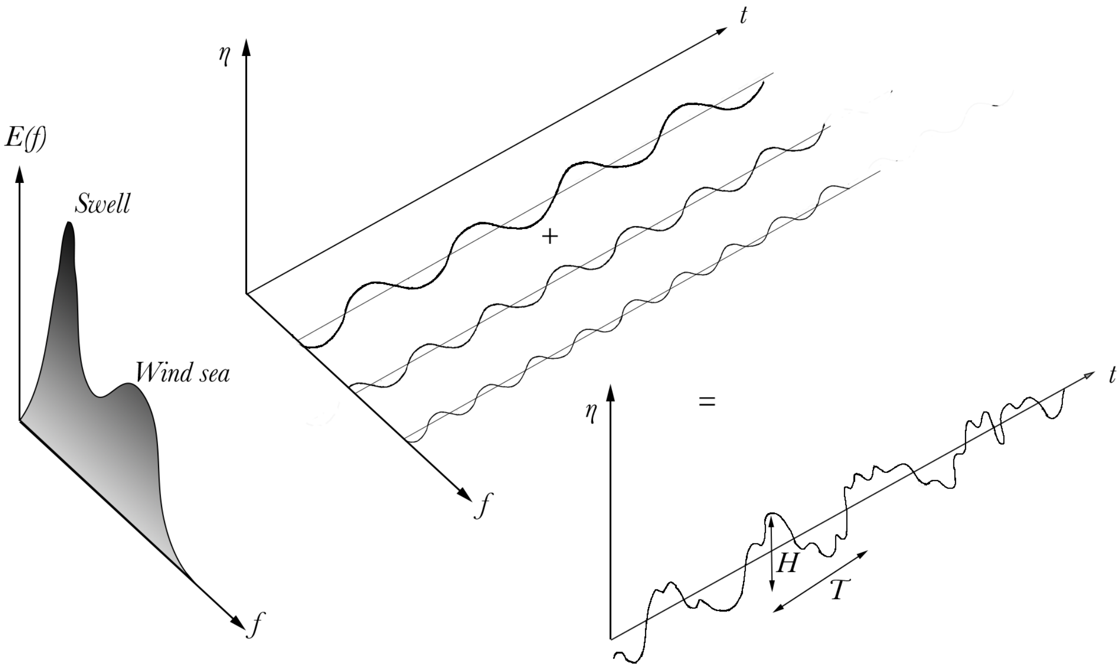

3D